EVALUATION OF VARIOUS OPERATING PARAMETERS ON AGRICULTURAL BOOMLESS NOZZLE SPRAY PATTERNS

By

MATTHEW BENJAMIN ROGERS

Bachelor of Science in Biosystems Engineering

Oklahoma State University

Stillwater, Oklahoma

2015

Submitted to the Faculty of the
Graduate College of the
Oklahoma State University
in partial fulfillment of
the requirements for
the Degree of
MASTER OF SCIENCE
July, 2017

EVALUATION OF VARIOUS OPERATING

PARAMETERS ON AGRICULTURAL BOOMLESS

NOZZLE SPRAY PATTERNS

Thesis Approved:

Dr. John Long

Thesis Adviser

Dr. Paul Weckler

Dr. Randy Taylor

ACKNOWLEDGEMENTS

This thesis has been a challenge and a learning experience for me, and it would not have been possible without the support of my committee, family, and friends. Every bit of support is appreciated and did not come unnoticed. Thank you to everyone who helped me along the way.

Name: MATTHEW BENJAMIN ROGERS

Date of Degree: JULY, 2017

Title of Study: EVALUATION OF VARIOUS OPERATING PARAMETERS ON AGRICULTURAL BOOMLESS NOZZLE SPRAY PATTERNS

Major Field: BIOSYSTEMS ENGINEERING

Abstract: Boomless Nozzles, a type of agricultural nozzle used for spraying pastures and roadsides, are characterized by the lack of booms. Booms provide even spacing of multiple smaller pattern nozzles to ensure even application across large swaths. In place of a boom, boomless nozzles make use of nozzle design and pressure to spray swaths of advertised widths between 20 and 58 feet. Boomless nozzles can be a single nozzle, a nozzle pair, or a cluster of nozzles that are usually mounted at the midpoint of the vehicle. The wide spray patterns that characterize boomless nozzles may allow for the influence of environmental or operational effects. The effects of wind, tractor speed, tractor pressure, and nozzle design on boomless relative deposition spray patterns were investigated. Nozzles were mounted on a tractor sprayer filled with a water and Rhodamine dye mixture. The tractor with the operating sprayer was driven over clean cotton string, allowing the string to absorb the Rhodamine dye mixture across the spray swath. The pressure of the sprayer as well as the speed of the tractor were varied. The tractor was driven indoors and outdoors. The strings were then processed through a reel and pulley system attached to a fluorometer, yielding a relative spray deposition pattern. These spray deposition patterns were then analyzed for a coefficient of variation, Christiansen's Uniformity Coefficient, overall width, effective width, area, width offset, and ratio skew. Some of these independent variables were statistically analyzed for significant effects and/or interactions of changing the speed, pressure, location, or nozzle. Statistically significant effects and interactions were observed.

TABLE OF CONTENTS

Chapter Page

LIST OF TABLES

Table Page

LIST OF FIGURES

Figure Page

CHAPTER I

INTRODUCTION

Boomless nozzles are used in areas where using boomed sprayers can be cumbersome. Boomless nozzles are easy to install, which leads to the popularity of this type of nozzle. XT boomless nozzles are Pentair's second most popular nozzle globally in dollar volume (Gary James, Pentair, personal communication, 13 April 2017). 70% of pasture sprayers sold by Wylie Sprayers in Oklahoma are boomless (Mickey O'Neill, Wylie Spray Center, Oklahoma City, personal communication, 17 April 2017). TeeJet reports steady XP and 5880 BoomJet nozzle sales during the previous six years prior to 2017 (Tim Stuenkel, TeeJet Technologies, personal communication, 17 April 2017). This communication confirms this nozzle popularity and shows why research on these nozzles is important. The boomless nozzles of this proposed study use an advertised spray width between 20 and 52 feet to eliminate the need for multiple nozzles on a boom. Due to these wide patterns, wind can be a factor in changing the resultant patterns. Drift studies have been evaluated primarily for boomed nozzles, leaving boomless nozzle pattern research an area of need. Other factors, such as nozzle pressure and tractor speed can also change spray patterns. If users of boomless nozzles can better understand how pressure, tractor speed, and wind can change the spray patterns of the nozzles, better spraying practices can be

implemented. This can lead to better pastures, money saved, and less drift which reduces harmful environmental impacts. Boomless nozzles spray in an arcing pattern to substitute for the lack of a boom. These spray patterns can be adjusted for width via the sprayer pressure which also changes the flow rate. Tractor speed may also change spray pattern width. Having a wide spray pattern compared to a boomed nozzle may lead to pattern variability from sprayer pressure, tractor speed, wind speed, or wind direction due to varying droplet size and the distance the droplets must travel. Changing spray pattern distribution and pattern width may reduce the effective application rate of the sprayer, therefore variables that change the spray patterns need to be investigated. This thesis lays out a method that evaluates the effects of nozzle pressure, nozzle model, tractor speed, wind speed, and wind direction on boomless nozzle spray patterns for different nozzles from various suppliers. String placed across the coverage area collects Rhodamine B dyed spray applied using a tractor-mounted, boomless sprayer. Three tractor speeds and three nozzles pressures are used according to the capabilities of the nozzle tested. Three replications of each speed and pressure combination are carried out indoors and three replications are carried out outdoors. Wind speed and direction are monitored continuously during outdoor testing to evaluate wind effects on the spray patterns. A completely randomized split-plot experimental design is utilized. Relationships between spray pattern and nozzle pressure, nozzle design, tractor speed, wind direction, and wind speed were evaluated. A coefficient of variation, Christiansen's uniformity coefficient, overall width, effective width, width offset, area, and skew of each spray pattern were calculated and analyzed.

Objective

The objective of this research was to determine the effects of nozzle pressure, tractor speed, wind, and nozzle model or type on boomless nozzle spray patterns. This information can contribute to developing better spraying application methods. In addition, insights from this study can be used by agricultural producers, nozzle manufacturers, and others concerned about boomless nozzle usage or spray drift.

Statement of Research Question

This research will determine how the spray pattern of the tested boomless nozzles changes with nozzle pressure, tractor speed, nozzle model, and testing location. After the effects of nozzle pressure, tractor speed, nozzle model, and wind are investigated outdoors, indoor testing will determine if the nozzles performed better an environment with no wind. Precise questions and objectives include:

- Develop a method for evaluating nozzle performance.
- Make use of Christiansen's Uniformity Coefficient and coefficient of variation to evaluate pattern uniformity.
- How does the overall width and effective width of each nozzle in this study compare to manufacturer's specifications?
- Does changing nozzle design, pressure, and vehicle speed effect performance?

Preliminary Testing

Boomless nozzles listed in Table 1 were installed on a three-point mounted 60 gallon Schaben Industries Sprayer. The sprayer was installed on a John Deere 4100 HST tractor. The nozzles were tested briefly (around 10 minutes) in the driveway of the Biosystems and Agricultural Engineering laboratory with varying pressure. A range of droplet sizes and swath widths were observed during preliminary testing that varied with nozzle type and pressure. Wind appeared to have an effect on swath width of the nozzles with larger swaths. It appeared that nozzle pattern relative distributions should be able to be obtained by driving the tractor-mounted sprayer over cotton string and measuring the fluorescence with a fluorometer.

During the summer of 2016, more extensive boomless nozzle testing was conducted using the Hypro Pentair XT 024 and TeeJet BoomJet 5880. Cotton string was placed across the parking lot of the Biosystems and Agricultural Engineering parking and the tractor was driven over the string using a system of boards and ramps while the nozzles were spraying Rhodamine B

dyed water. Wind conditions were also recorded. The XT 024 was tested at 40, 50, and 60 pounds per square inch (PSI) while the 5880 was tested at 20, 30, and 40 PSI. Tractor speed was maintained at 5 miles per hour (MPH). The dyed string was analyzed using WRK of Arkansas software designed for use with a Turner Model 111 fluorometer. The software prints a relative deposition of spray graph for each cotton string. Preliminary results shown in Figures 1 and 2 demonstrated varying relative deposition patterns, possibly related to nozzle, pressure, and wind conditions. It was decided that further research would be done to investigate these possibilities, while also varying tractor speed.

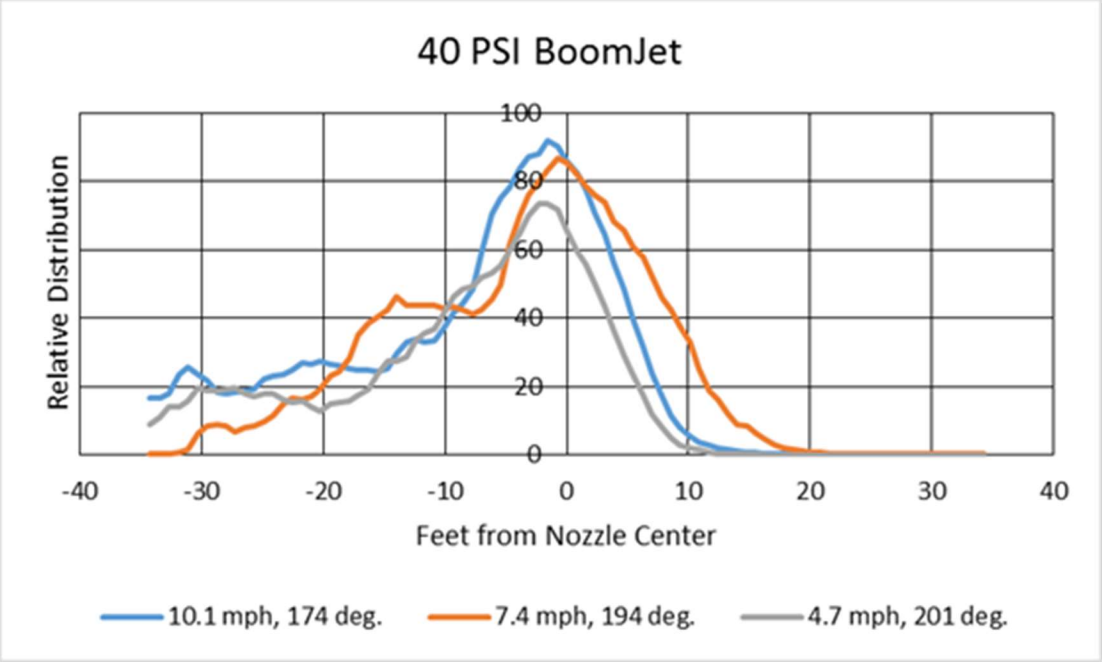

Figure 1. Selected preliminary testing results of the BoomJet 5880.

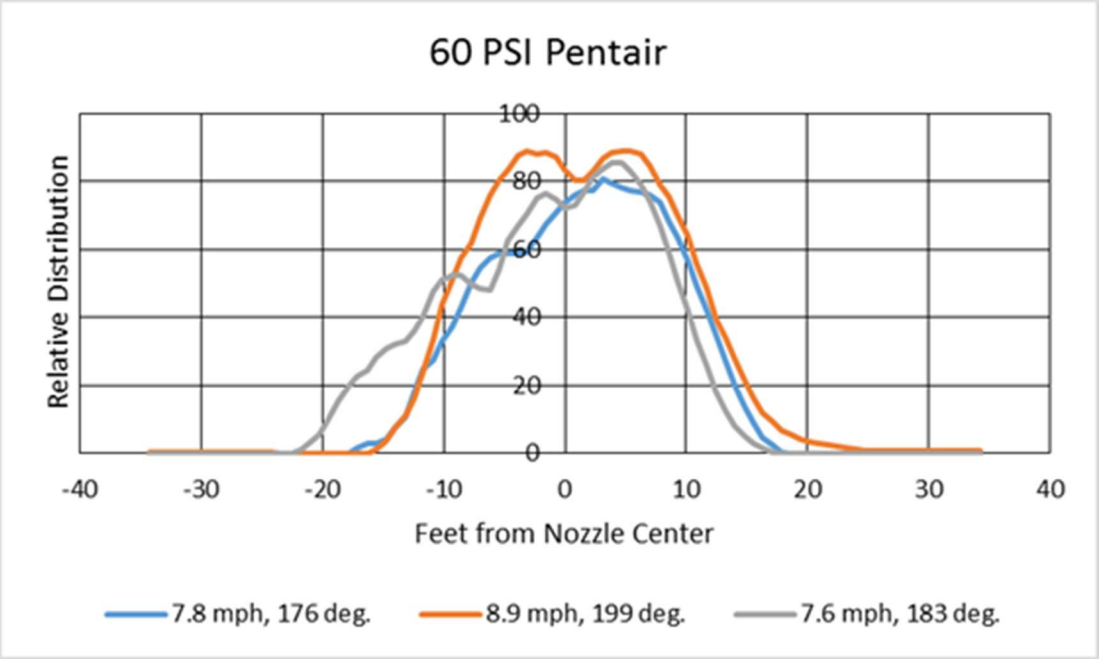

Figure 2. Selected preliminary testing results of the Hypro Pentair XT 024.

CHAPTER II

LITERATURE REVIEW

Whitney and Roth (1985) compared the fluorometric response of cotton floss and paper tape collectors when sprayed with Rhodamine B dye using flooding and fan nozzles from Spraying Systems nozzle models TKSS.75 and 650017. The fluorometric response of the floss and tape were evaluated using a Sequoia-Turner model 112 fluorometer. The fluorometric response of the cotton floss string was determined to be equal to or better than the paper tape. A correlation coefficient of .94 was obtained by plotting the net mean fluorescence of the treatments tested for the floss string and the paper tape. The correlation coefficient indicates a direct relationship between the string and tape measurement methods. Tests were also conducted to determine that the optimum dye concentration is 300 parts per million (ppm) for string testing. This study shows that the fluorometric response of string can be used to measure the net mean fluorescence. The net mean fluorescence can be used to measure the relative spray pattern flow distribution. Aspects of this study will be used during research proposed in this paper when evaluating spray patterns of the boomless nozzles. In the first two parts of a five part study, Nuyttens et al. (2006) evaluated the effects of meteorological conditions and spray application technique on agricultural sprayer drift. A reference spray was defined, and horizontal drift

Collectors (.25 by .25 meter type 751 Machery-Nachel filter paper) were positioned downwind from the reference spray. The reference spray was conducted with a Hardi Commander Twin Force trailed sprayer with a 27 meter boom, nozzle spacing of .50 meter, and a 3200 liter tank. Nozzles were at a .50 meter height, three bar pressure, and conformed to the ISO 110 03 standard. Tractor speed was 8 kilometers per hour (km/hr). These parameters resulted in a 180 liter per hectare (L/ha) application rate. Testing was conducted in a flat meadow while meteorological conditions were monitored every three seconds using a Campbell Scientific weather station. Brilliant Sulfo Flavine was used as the tracer. 27 reference sprays were conducted along three spray lines that were marked. The spray line chosen was the line closest to being perpendicular to wind direction. Eight collectors were placed on each line, for a total of 24 collectors. Each spray line made use of eight horizontal collectors positioned downwind. The 27 reference sprayings that were conducted resulted in a total of 648 measurements. From reading the fluorescence on the collectors and using the collection area, spray volume, tracer concentration, and a calibration factor, drift deposition and drift percentage were calculated. A relationship between spray drift percentage and drift distance parallel to the wind direction, dew-point temperature, average wind speed at 3.25 m height, average relative humidity, and average temperature was developed using non-linear regression statistics. The relationship had a coefficient of determination value of .873. This study highlights a useful method for measuring drift and relating it to wind, and shows that wind is an important factor to consider when evaluating nozzles.

Dibble et al. (1958) compared the effectiveness of boomed and boomless sprayers in the application of Malathion to kill spotted alfalfa aphids. Specific nozzles were not given. The boomless nozzles were compared to a 30 feet spray boom with flat fan nozzles. The boomed setup had the same application rate as the boomless nozzles. Spotted aphids were counted at three feet intervals across the spray pattern width. Four replications were made. Counts were made at four locations per replication. Occasional gusts of wind were not measured. Boomed nozzles killed more aphids per stem on average and offered a less sporadic spray distribution compared to

boomless nozzles. Wind effects were also evaluated for the boomed and boomless nozzles. Dyed water spray was collected on stainless steel plates and analyzed. The maximum distribution point of the boomless nozzles ranged from 1.2-2.0 times the average spray distribution level compared to 1.3-1.4 for the boomed sprayers in wind velocities ranging from 1.7-5.4 miles per hour. Crosswinds were found to change boomless swath width by as much as three feet per mph. This research confirms a need to further investigate wind effects on boomless nozzles.

Miller (1990) investigated spray distribution patterns of three boomless nozzles using cups to collect the water spray at tractor passes between two and three mph. Nozzles evaluated were the BoomJet 5880, Radiarc, and Boom Buster. Pressure was maintained at 20 pounds per square inch (psi) for the Boomjet and 40 psi for the Radiarc and Boom Buster. Application rate was measured by draping plastic over the nozzles and collecting and measuring the runoff in a pail. Testing was performed outdoors at Auburn University where buildings partially blocked the wind. Testing was suspended when wind gusts were over six mph. The plastic cups were positioned at one to three feet intervals near the tractor and two feet intervals past the tractor. The cups went out to 32 feet to each side of the tractor. 15 tractor passes were used for each measurement. Coefficients of variation (CVs) were calculated for each nozzle configuration. In the standard setups, the Boomjet, Radiarc, and Boom Buster had CVs of 61-65%, 18%, and 26%. The effective swath width of the Boomjet was observed to decrease as the ground speed increased. It was also observed that wind gusts over 10 mph greatly increased the swath variability. These two observations need further testing. The boomless nozzles were sensitive to horizontal alignment, with changes causing large differences in spray patterns. Terrain was observed to also play a factor in spray patterns. This research shows that patterns of boomless nozzles vary and more investigation into what causes the variability is needed, in addition to investigating wind effects on the patterns. This research also made use of coefficient of variation as a measuring factor of nozzle performance. CVs were used in the research conducted for this thesis.

Wolf and Peterson (2009) evaluated the TeeJet BoomJet, Hypro Boom Extender, Evergreen Boom Buster, and Wilger Combo-Jet for pattern quality, width, droplet size range, and coverage effectiveness. Two herbicides, glyphosate and paraquat, were applied to a wheat crop with each nozzle. The nozzles were tested with a 12 volt, 45 psi, 3.6 gallon per minute (gpm) pump mounted to an ATV. The spraying was conducted on the wheat crop at four to five inches tall (prior to jointing) and 24 to 30 inches tall (after jointing). Treatments were repeated three times. Water sensitive paper placed across the spray width collected spray droplets which were analyzed with computer software using a scanner. Swath width was found to be less than manufacturers' ratings. Pattern uniformity for the paraquat trials varied between five and eight for the nozzles on a relative scale of zero to ten. Wind direction and spray height may have affected the results from the study. This study shows more research is needed to investigate changes in effective swath width and demonstrates the variation in spray pattern between boomless nozzles. In addition, the research in this thesis also compared manufacturer's swath width ratings to tested swath width ratings.

Kees (2008) tested a constant application rate ATV sprayer with boomless and boomed nozzles. The spray tank was a 13 gallon C-Dax Spray Rider. A Spray-Mate II control console regulated the pressure and pump flow. An Astro II GPS speed sensor sent speed signals to the controller. The pump was a SHURflo 2088 rated at 3.6 gpm and 25 psi. Nozzles evaluated were a Boominator 1400FM boomless nozzle mounted at a 45 degree angle to the ground and Turbo TeeJet TT11002 fan nozzles mounted on a boom. Five TeeJet nozzles were used making a 100 inch spray swath. A five percent red food dye solution was sprayed on white test cards set at six inches above the ground. Cards were placed at 2.5 feet apart for 15 feet from the sprayer centerline. Testing was conducted when wind speed was less than four mph. REMSpC Stainalysis was used for analyzing data. The volume density of the boomless nozzle experienced a sharper peak in the middle of the spray pattern at 4.5 mph compared to the boom nozzle. However, the target rate and width of the boom nozzle was 15 gallons per acre (gpa) and 8.5 feet compared to

13 gpa and 22 feet for the boomless nozzle, so the testing parameters were not the same. This research shows a need for more extensive testing on boomless nozzles to look at the distribution of spray patterns and how they change with travel speed and pump pressure.

Smith and Plummer (1984) evaluated broadcast spray nozzles using both a spray table and field tests. The sprayers were set up on the spray table at different angles and crosswinds to simulate field conditions. Nozzles evaluated were models 8002, 8004, 8002LP, and 8004LP. The spray table was 2.44 meters wide and 1.22 meters deep. 80 channels that drained into 80 graduated cylinders of 50 milliliters (mL) each were set below the spray table to measure spray volume. To simulate wind and ground speed conditions, a wind tunnel was superimposed on top of the spray table. A .62 meter diameter propeller fan was used to draw air through the wind tunnel. Honeycomb sectioning was installed between the fan and the wind tunnel to reduce vorticity. A range of air velocities and spraying angles were evaluated. A computer program was used to mathematically overlap the calculated spray deposits for the different nozzle spacing. CVs were calculated for each nozzle setup that was evaluated, and the wind velocity vector was found to not have a consistent effect on CV values. Field tests were also run in an open grass area to compare laboratory results. Brilliant Sulfo falvine dye was dissolved in the water spray to measure fluorescence. Polyester film targets were used. Four TK-10, four RA-15, and eight 8004 nozzles were evaluated. No evidence was found that laboratory tests were indicative of field tests. The authors recommend that laboratory testing not be used as the only basis for field spraying recommendations. This paper shows the need to continue nozzle field testing and not rely only on laboratory data. This test was contradictory to the results found in the research presented in this thesis, which showed that wind did have an impact on CVs.

Krishnan et al. (1993) investigated the effects of sprayer bounce, wind speed, and wind direction on spray pattern displacement of TJ60-8004 fan nozzles from Spraying Systems Co. The nozzle was studied using a spray patternator. Four pressures, 139, 208.5, 312.8, and 382.3 kilopascals (kPa) and two sprayer bounce conditions of .2 meter and .4 meter amplitude at a

frequency of 1 Hertz (Hz) were used. Two .61 meter axial fans simulated headwinds and a .91 meter axial fan simulated crosswinds. Wind conditions were a 2.68 meter per second (m/s) crosswind, a 2.68 m/s crosswind with a 2.23 m/s headwind, a 4.46 m/s crosswind, and a 4.46 m/s crosswind with a 2.23 m/s headwind. Both wind speed and direction, as well as their interaction, were found to have significant effects ($P < .05$) on spray pattern displacement values at 139 kPa. At 208 kPa and 312 kPa, sprayer bounce, wind speed, wind direction, and wind speed and wind direction interaction had significant effects ($P < .05$) on spray pattern displacement values. At 382.3 kPa, sprayer bounce, wind speed, wind direction, sprayer bounce and wind speed interaction, and wind speed and wind direction interaction had significant effects ($P < .05$) on spray pattern displacement values. This study shows that wind conditions in addition to sprayer bounce change spraying quality at different pressures.

ASABE Standard S327.4 (July 2012) in section 4.13 describes a skewed pattern, "One that is non-symmetrical about the center of the applicator with no outside influence." The standard is labeled as "Terminology and Definitions for Application of Crop or Forestry Production and Protection Agents." Therefore, this standard is applicable for boomless nozzles, although they are not specifically mentioned. This thesis studies skewed patterns, specifically referred to as "ratio skew" in this thesis.

Another standard, ASABE S341.4 (Dec. 2009) describes distribution uniformity for granular broadcast spreaders. This standard defines the effective swath width to be the distance between the points on either side of the swath where the deposition rate equals half the effective application rate. This study described in this thesis uses a similar method, but instead uses the area where the relative deposition is half of the maximum deposition.

CHAPTER III

METHODOLOGY

General Overview

Seven boomless nozzles of different designs mounted on a tractor sprayer were evaluated at changing locations, pressures, and tractor speeds to evaluate the effects of those factors on the spray patterns. See table 1 for the list of nozzles tested. To evaluate these effects, testing was conducted indoors and outdoors, creating a split-plot design. Pressure, speed, and nozzles were changed at each location (referred to as setting in some instances) in a completely randomized manner. Previous research has shown that the fluorometric response on dyed string is highly correlated to the application rate of a sprayer nozzle (Whitney and Roth). Therefore, a Turner model 111 fluorometer was used to evaluate the boomless nozzle sprayer patterns on six-strand cotton string (Figure 3). A tractor was driven across an 80-foot long string while operating a boomless nozzle emitting fluorescent-dyed water. The tractor path was perpendicular to the string, and the tractor was driven across the string midpoint. To prevent the ground and tractor tires from contaminating or damaging the string, the string was raised seven inches off the ground by fastening it to screws secured to wooden blocks at each end of the string. A wooden platform eight inches from the ground with a two-inch gap between sections was

constructed to allow the tractor to drive over string. The two-inch gap section was where the string went through the platform. While testing outdoors, wind speed and direction were recorded to evaluate those effects on spray patterns. After testing was completed, the fluorometer was used to evaluate relative deposition of flow rate that the nozzles deposited across the strings.

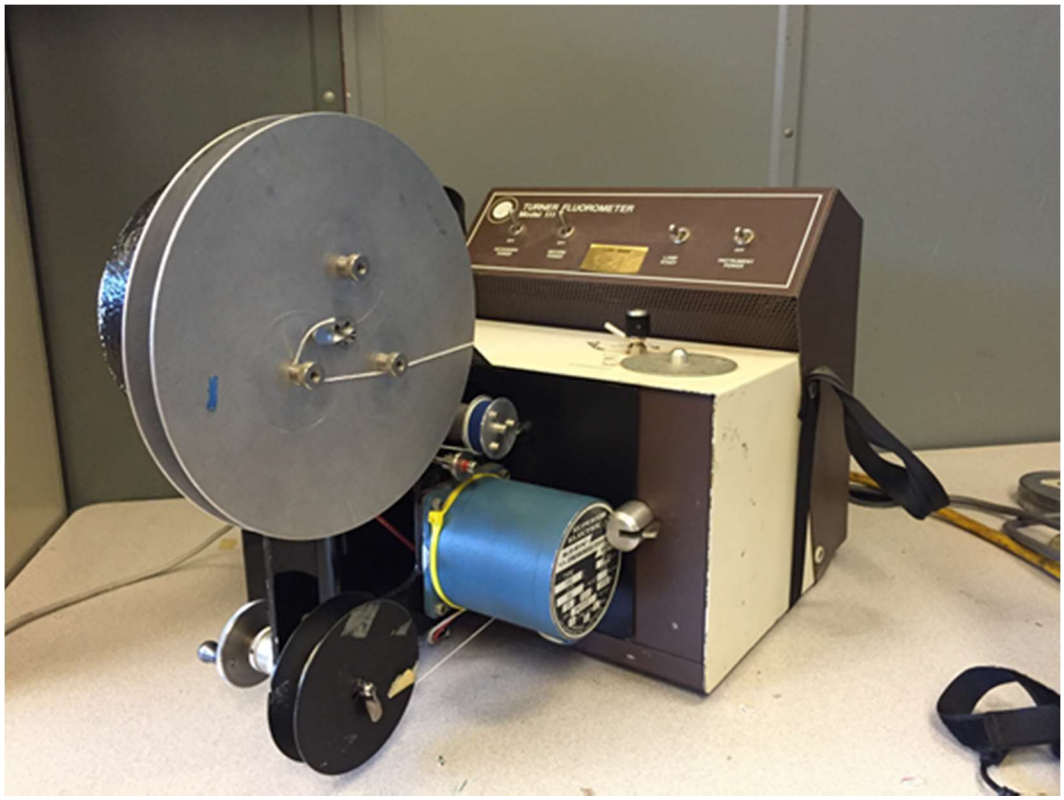

Figure 3. Turner Model 111 fluorometer with special "string analysis door" used to measure relative net mean fluorescence of the spray pattern across the string.

Experimental Design

The experimental design was a split plot design, with the setting (or location, either inside or outside) as the main plot. Nozzle model, nozzle pressure, and tractor speed were completely randomized within each plot. A split plot design was chosen because it allows for factors that are easy to manipulate to be randomized, while the difficult factor can be split between plots. Furthermore, because each setting is completely randomized, each setting can be analyzed separately as a completely randomized design. Moreover, the same can be said for each the effect

of speed and pressure on each individual nozzle model, as each individual nozzle can be evaluated by setting as a completely randomized design. The experiment was analyzed at times by breaking the nozzles into two groups, as the 5880, KLC 18, and KLC 36 had to be tested at four, six, and eight mph and 20, 30, and 40 psi while the other nozzles were able to be tested at six, eight, and ten mph and 40, 50, and 60 psi. These different ranges of nozzle test parameters were due to nozzle limitations placed by the manufacturers. In other instances, the experiment was analyzed by nozzle model.

Before testing was started, the factors within each plot were completely randomized using the random number generator in Microsoft Excel. Each possible factorial combination was written out three times to allow for the three replications. The random number generator placed a random number next to each factorial combination and the replications, and then the order was sorted from greatest to least. This randomization procedure generated the order that the experiment was conducted, first outside and then inside. When the experiment was moved inside, the data was again randomized, so it was conducted in a different order than it was conducted outside. Testing was conducted outside first due to time constraints. See Table 1 for the tested factors for each nozzle. Figure 4 shows the nozzles tested.

Table 1. Planned testing details for each nozzle that was tested. The BoomJet was not tested due to available equipment limitations. See references for citations.

Brand	Model	Type	Pressure (PSI)	Tractor Speed (MPH)	Nozzle Height (In.)	Reps.	Flow Rate (GPM)
Teejet	XP 25	High	40, 50, 60	6, 8, 10	36	3	5.0-6.0
Teejet	XP 40	High	40, 50, 60	6, 8, 10	36	3	8.0-10
Pentair	XT024	High	40, 50, 60	6, 8, 10	36	3	4.8-5.8
TurboDrop	Boom40TD	High	40, 50, 60	6, 8, 10	36	3	4.0-5.0
Hamilton	6542-1	High	40, 50, 60	6, 8, 10	36	3	5.9-7.1
Fieldjet	1/4-KLC-18	Low	20, 30, 40	4, 6, 8	36	3	2.5-3.6
Fieldjet	1/4-KLC-36	Low	20, 30, 40	4, 6, 8	36	3	5.1-7.2
Boomjet	5880-3/4-2TOC20	Low	20, 30, 40	4, 6, 8	36	3	6.1-8.6

Figure 4. Starting from top, both rows left to right: KLC 18, KLC 36, Hamilton, XT 024, 5880, XP 25, XP 40, Boom40TD.

Wooden Platform

A wooden platform was constructed for testing trials. Two eight feet (ft.) long sections placed in parallel with each other spaced the width of the tractor were used along with two twelve feet long sections arranged directly in line with the 8-ft. sections. Between the 8-ft. section and the twelve-ft. section a two-inch (in.) gap was left in the platform. Cotton string was stretched across the testing area perpendicular to the direction the tractor traveled and through the 2-in. gap

in the wooden platform. The string was stretched 80 feet across, with the midpoint being in the midpoint of the platform where the tractor was driven. The string was secured at each end to wooden blocks that had a screw in the top. The string was fastened by wrapping it around a screw, allowing the string to hang in tension seven inches from the ground. The wooden platform was constructed using blocks that were two feet long each, pictured in figure 5. The block sections were constructed using 4 x 4 inch nominal sized lumber in the middle sections and 2 x 12 inch nominal sized lumber were used for the top and the bottom. The blocks were then placed directly in front of each other to make the 8-ft. sections and the twelve-ft. sections. More 2 x 12 inch nominal boards were screwed over the top of the platform to stabilize the platform for when the tractor drove across it. After the top stabilizing boards were installed, the overall platform height was eight inches. The distance on center (OC) that the two rows of platforms were placed was 29 inches (the track width of the tractor). At the end of each wooden platform, wooden ramps (8 ft. sections of 2 x 12 inch nominal) were screwed into the platform to allow the tractor to drive onto and off the platform. Figure 6 shows the finished wooden platform.

Figure 5. One of the blocks used to construct the wooden platform.

Figure 6. Wooden platform used during both indoor and outdoor testing being shown in the testing position.

Outdoor Testing and Location

Outdoor testing was conducted on Oklahoma State University Department of Plant and Soil Science property located on the west side of Oklahoma Highway 86, latitude and longitude coordinates 36.141360, -97.283676. Testing was conducted during clear weather conditions with no precipitation. Temperatures varied between 25° F and 60°F. However, temperature was not considered a variable that would be controlled or monitored for this research. In addition, testing was conducted only during conditions when the anemometer of the weather station was constantly rotating to indicate a wind presence.

Before outdoor testing was started, the wooden driving platform was installed. The platform was installed from east to west in the manner as discussed in the wooden platform

section of this thesis. This platform was left in the same position day to day, and was not removed from the field until all outdoor testing was completed. A test run occurred when the tractor was continuously driven over the platform from east to west with the nozzle operating until the tractor had completely exited the ramp. A flag was placed in the middle of the platform which is where the midpoint of the string was measured. The operator focused the midpoint of the tractor on the flag to have as consistent runs as possible.

A procedure was developed due to ice accumulation on the ramps. This was noticed during a couple of days. If any ice was noticed, testing was stopped because the tractor would easily slide off the ramp. If the tractor slid off the ramp during a test run, the string was thrown away and the run was repeated when outside conditions were safer. Ice was not noticed on any nozzles, but the nozzles were checked for ice and the nozzles were run for a few seconds while the pressure setting were adjusted. This served as another check against ice. Ice could possibly change the nozzle spray patterns and would be undesirable for this experiment. Testing was conducted from December 18, 2016 through January 13, 2017.

Indoor Testing

Indoor testing was conducted at the Oklahoma State University Animal Science Arena (Totusek Arena). Overhead fans were turned off but a couple garage doors were left cracked for ventilation and to prevent carbon monoxide buildup. The arena was large enough to allow for the tractor to gain enough speed, complete the run, and slow down. In addition, there was enough room for the operator to drive the tractor around the 80 feet of string after a run was completed to reset the tractor and the nozzles. Testing was completed inside in the same manner as it was completed outside, with the exception that weather data was not recorded. The arena floor consisted of smooth bare-soil that had been smoothed via a tractor before testing was begun. The arena floor was not smoothed again until testing was completed. In addition, the wooden platform was not removed until all testing was completed. All runs were conducted in a completely randomized order, different from the outdoor runs. Indoor testing is shown in Figure 7.

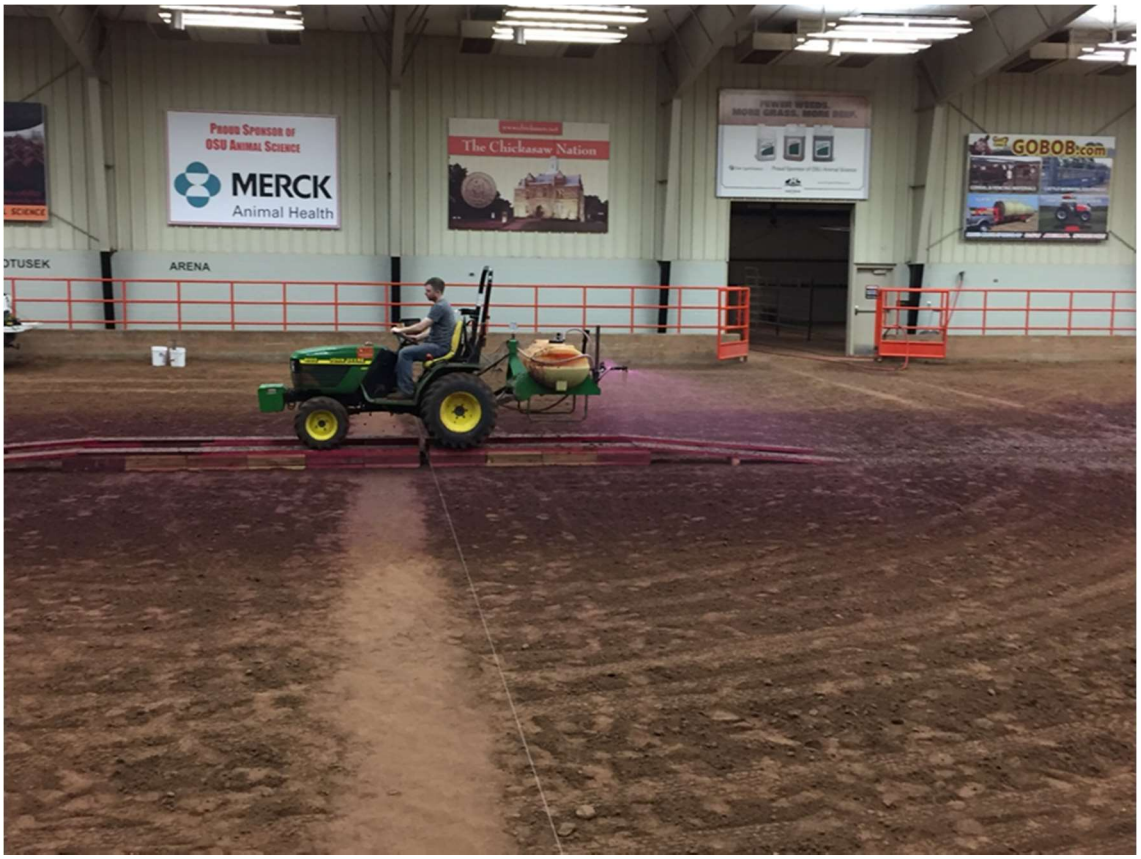

Figure 7. Indoor testing of the nozzles.

Weather Station

In order to evaluate wind effects on the boomless sprayer patterns, a weather station was utilized to monitor wind conditions during outdoor testing. Wind speed and direction were recorded every second using a SparkFun Electronics SEN-08942 weather meter. The Weather Meter consists of a wind vane, anemometer, and rainfall gauge. Only the wind vane and anemometer were utilized. The wind vane and anemometer were connected to a SparkFun Electronics DEV-13975 Redboard via a SparkFun DEV-13956 weather shield. The weather shield included a GP-365T GPS receiver. This receiver was used to output a time stamp every instant that weather information was outputted from the weather station. The Redboard is a microcontroller that is programmed using Arduino programming language using the Arduino graphical user interface on a personal computer. The Redboard also inputted all incoming data into the computer. Programming was uploaded to the Redboard using code that was available via

the SparkFun website. A code that worked but did not include GPS data had to be merged with a code that did not fully function but the GPS function worked. The fully modified code is copied in the appendix, and due to the modification it cannot be found in its current form online. Arduino 1.6.7 was the Arduino software that was used. After the Arduino code was uploaded to the Redboard, the serial monitor in the Arduino software package was opened to ensure that all components of the weather station were fully operational. The serial monitor was then closed and a Python 2.7 script was opened to store the data from the weather station to a file on the computer. The Python script is available in the appendix. Figure 8 shows the weather station.

Figure 8. Weather station setup.

The weather station was setup directly in front of the tracks, approximately 40 feet in front from the end of the tractor ramp. This distance gave the tractor operator plenty of time to stop the tractor from endangering the weather station. The weather station wind vane and anemometer were placed two meters from the ground. Two meters was chosen due to the

availability of data at two meters from the Mesonet weather system of Oklahoma, in the case that weather data needs to be compared to Mesonet data or project repeatability using the Mesonet station instead of a portable weather station. The tractor was driven from east to west directly toward the weather station. The way the weather station was programmed indicated that wind coming from the east would indicate 90°. Wind coming from the north indicated 0°. Wind coming from the west indicated 270°. Overall, the wind vane degree values ranged from 0° to 360°, with sixteen divisions. 0° and 360° are the same value, so they all were programmed to be 0°. Figure 10 shows a setup overview.

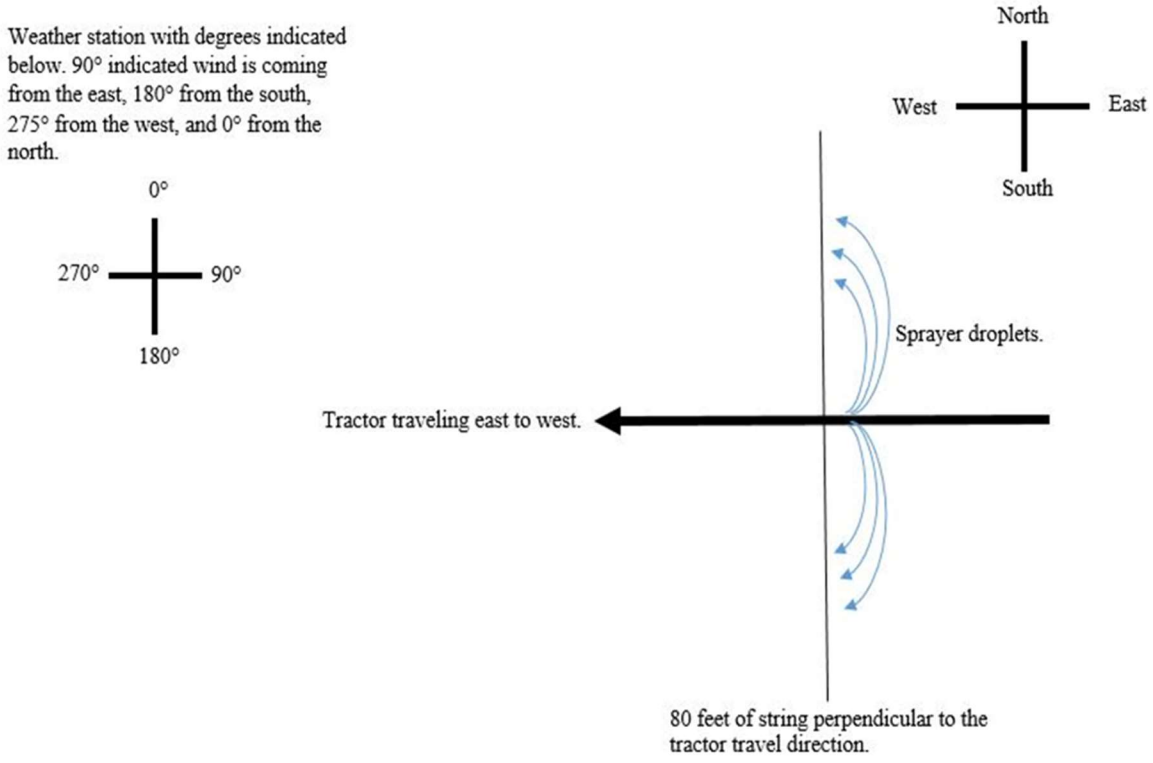

Figure 10. Overall outdoor setup and weather station overview.

During each sprayer run, as the tractor was driven across the string the exact minute as indicated by a cell phone was recorded by hand by a research assistant. After testing, the hand-recorded minutes were matched with the time stamps from the weather station GPS. The average wind North and East coefficients were calculated for the average of three minutes for each run.

The average was taken for the minute before the run, the exact run minute, and the minute after the run. N and E coefficients were calculated using the following formulas:

$$N = V * \cos\theta$$

$$E = V * \sin\theta$$

Where N is the north to south wind component in miles per hour (mph),

E is the east to west wind component in mph,

V is the wind speed as recorded in mph,

And Ɵ is the wind direction as recorded in degrees.

For each recorded data point, the wind components were calculated using Microsoft Excel. These components were then averaged. In order to reduce math errors, the positive or negative signs of the components were not adjusted when the equations were applied for the wind vane angle ranging from 0° to 360°. Therefore, a positive N component indicated the wind is coming from the north and traveling south, and a positive E component means the wind is traveling from the east and heading west. The weather station was programmed to record at 1 hertz.

Sprayer

A John Deere 4100 hydrostatic transmission tractor was used during testing along with a Schaben 60 gallon sprayer tank mounted on the three-point hitch. The sprayer was plumbed with two strainers, a 50 mesh directly after the pump and a 50 mesh before the pump. Nozzles that were used are listed in table 1. The Pentair requires two opposing nozzles to spray a full left and right side pattern; therefore a tee pipe was needed. In order to ensure proper setup, a Boom X Tender Tee/Swivel Kit was obtained from Pentair that was specifically designed to work with the nozzles. See Figure 10 for the sprayer plumbing setup. Nozzles were mounted 36 inches above the string, and were fine tuned for each replication using an adjustable mount built for the nozzles. The sprayer tank was filled with a concentration of 300 ppm purple Rhodamine B dye. A mark was placed on the tank where a full bottle of dye could be put in the tank and the remainder

of the tank was filled using water up to that mark. After the tank was filled with dye, the sprayer pump was turned on with nozzle off to agitate the water until the dye appeared to be thoroughly mixed. The nozzle was adjusted to the correct pressure before each run using a pressure gauge built into the sprayer system plumbing. The pressure was manually adjusted using a throttling valve. Additionally, the nozzle height was fine-tuned using the adjustable mount and a measuring stick before each replication. Figure 11 shows the actual sprayer used for testing.

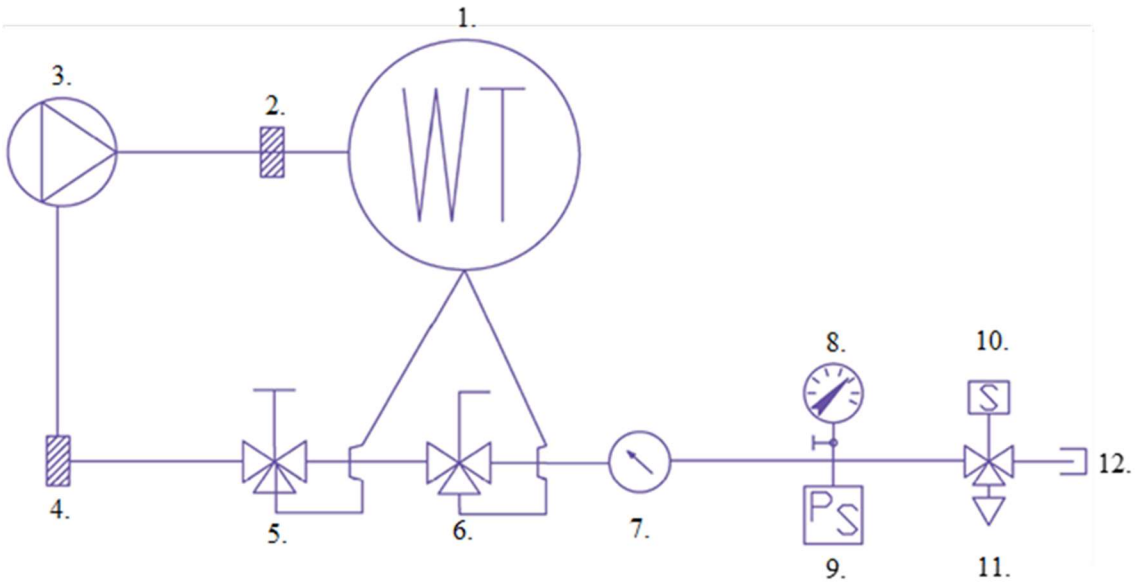

Figure 10. Plumbing schematic of the sprayer used for testing. (1.) 60 gallon spray tank, (2.) 50 mesh strainer, (3.) Hypro 7560 XL roller pump driven by the rear pto of the tractor, (4.) 50 mesh strainer, (5.) pressure relief valve with excess fluid routed back to tank which broke before testing and was replaced with a capped off with a tee, (6.) throttling valve with excess fluid routed back to tank, (7.) Omega FTB4607 flow meter that was inoperable during testing, (8.) analog pressure gauge, (9.) digital pressure gauge connected to National Instruments USB 6008 DAQ, (10.) three-way solenoid valve that is routed to the nozzle with the other end capped off, (11.) boomless nozzle, (12.) pipe cap.

Figure 11. Sprayer plumbing.

Tractor Speed

Before the testing procedure was started, the John Deere 4100 hydrostatic tractor was prepared for testing at preset speeds, as opposed to the continuous range of speeds allowed by the hydrostatic transmission. A bracket and adjustable bolt were installed below the hydrostatic pedal of the tractor. The bolt could be adjusted to prevent the pedal from being fully depressed. Marks along the bracket were made where the end of the bolt indicated the tractor speed. The marks were determined by driving the tractor on a relatively level sidewalk along Hall of Fame Road in Stillwater in front of the Biosystems and Agricultural Engineering Laboratory. A Garmin Nuvi 1450 GPS system was placed on the tractor, and the GPS speed output was used to determine the speed of the tractor to the nearest whole mile per hour. A mark was then made using a straight edge and a marker to line up the end of the bolt and the bracket. The straight edge was then used before each test run to adjust the screw and line it up with the mark for the particular tractor speed needed for the run. The speed apparatus is shown in Figure 12.

Figure 12. Speed adjustment apparatus.

String

String was the primary data collection tool used for the experiment. Before each run, six-strand cotton string was attached to screws on wood blocks on each end and stretched across the testing grounds and through the wooden platform 80 feet. An additional ten feet of unused string was left on the reel to protect it from the dye, but it was marked off to be used for zero calibrating the fluorometer. Each end of the 80-ft. sections used to collect data were marked with a different color marker. Strings were not cut until a collection reel was completely full. Keeping successive strings uncut made running strings through the fluorometer easier, as a new string did not have to be routed through the reels for each run. The analyzed sections of the strings were continuously reeled up by the fluorometer.

Data Collection

Data collection involved gathering data from the strings and from the weather station. Strings were reeled into either small collection reels during outdoor and indoor testing or a large collection reel during outdoor testing. During tractor runs, unused tractor strings were kept covered in a box away from the spraying. The large reel was used when small reels were no longer available. See Figure 13 and 14 for an image of the reels. However, all strings were transferred to the small reels for the string to be processed through the fluorometer. The string was reeled up from the north to the south during outdoor testing, meaning the south side was analyzed first going through the fluorometer. The south side of the strings are represented by the negative distance value on the relative deposition graphs. The indoor strings were reeled up from the same direction as outdoor strings relative to the direction of the tractor travel. This way the indoor data and the outdoor data is comparable. After strings were used for a test run, they were reeled up and covered by a box to protect them from spray drift. After all strings were collected, the string were then reeled through the fluorometer. The fluorometer graphed the relative deposition using a scale between zero and 100 as well as created a data file for the relative deposition per .72 feet of string. Before the fluorometer read the relative deposition on each string, the fluorometer automatically calibrated its software using a blank portion of string that was attached to the test run string. The fluorometer was setup with the primary filter door set to "30" and a .32 filter was utilized, along with a dark green colored glass. The "30" limits the filter door opening to 30% of its full open setting. The .32 filter allows 32% light to enter the opening. An amber colored glass and mirror were placed over the secondary filter door. See figures 15 through 19 for filter setup. The top relative fluorescence adjustment wheel that is set before each run and ranges between zero and 100 was set to five to ensure that relative deposition results would not fall below zero during calibration. A one inch mark on the string placed by the research assistant during outdoor and indoor sprayer testing indicated that the portion of string with sprayer dyed water on it was about to travel through the fluorometer. During calibration,

when that mark was seen by the operator before it went through the fluorometer door, the WRK of Arkansas software program was manually started and the fluorometer immediately began reading the fluorescence. The software utilized an encoder on the pulley system of the fluorometer door to measure distance on the string as the string is processed through the fluorometer. The program was started manually for every run by the fluorometer operator initializing a button on the software computer screen. This manual method of starting the program allows room for error per replication, and that error is accounted for in the split plot analysis model. However, error should be relatively consistent compared to if multiple people were running the fluorometer because only a single person operated the fluorometer for all runs. Figures 20 and 21 shows software screenshots.

Figure 13. Small reel used for string.

Figure 14. Large reel used for string.

Figure 15. Amber glass on secondary filter.

Figure 16. Mirror on secondary filter.

Figure 17. Primary filter door set to 30.

Figure 18. Green glass installed over primary filter.

Figure 19. .32 Filter on primary filter side.

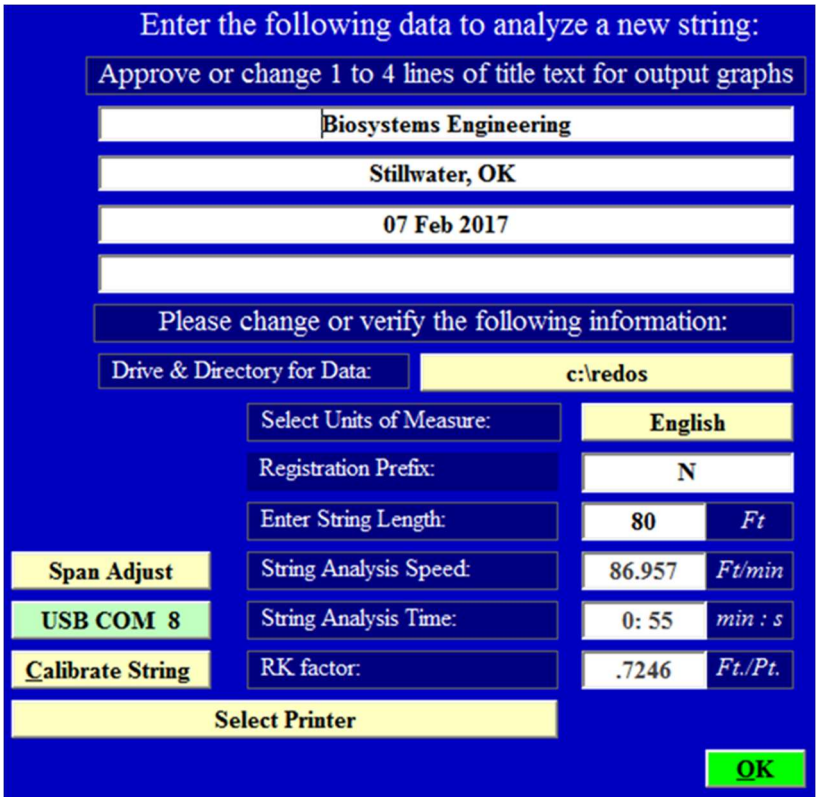

Figure 20. Screen shot of software parameters.

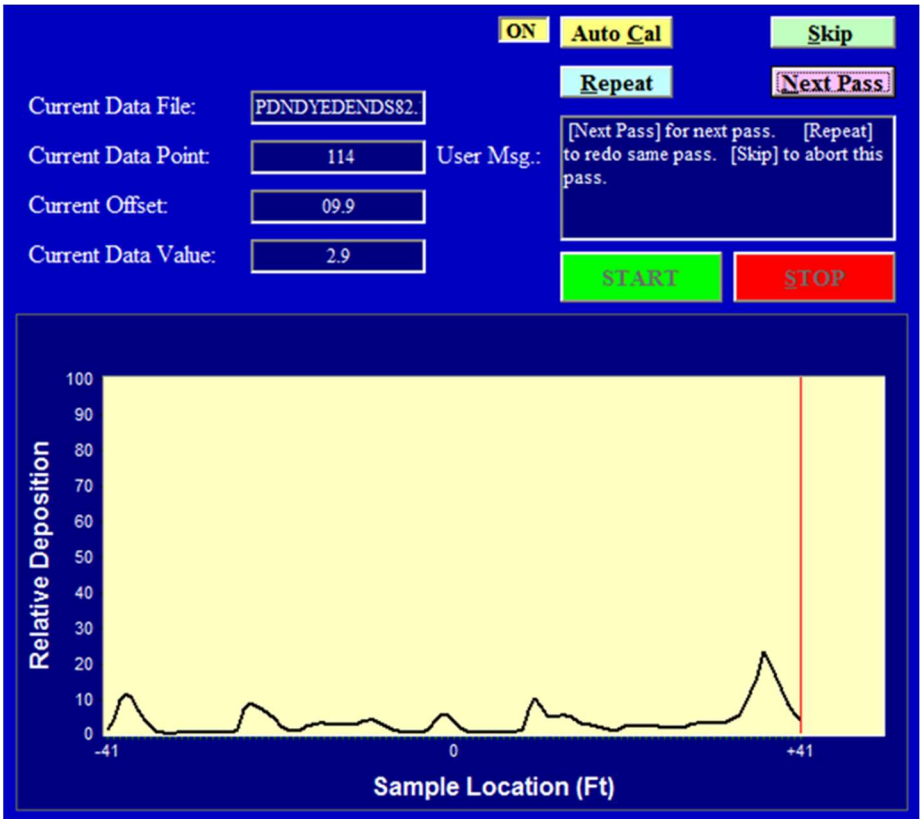

Figure 21. Screen shot of fluorometer output.

After fluorometer data were collected, certain variables for each run were calculated, including the overall width, width distance from center, area under the curve, and ratio skew. In addition, simulated overlap graphs were developed and analyzed. All of these values were calculated from what was arbitrarily defined to be the swath of the nozzle pattern for each run. These swaths varied from replication to replication, and the swaths were manually trimmed for each run's relative deposition dataset. The swaths were defined as the part of the dataset where the relative deposition versus width graph was largest in area and that did not go below .5 on the relative scale as generated by the fluorometer. This definition separated the swath data from the data that was generated either by the mark on the string made by the research assistant that indicated when the data portion of the string was beginning as well as parts on the string that contained fluorescence but were judged to be minuscule compared to the rest of the data. This defined portion of the string data is the portion of the data that was used for analysis in the split-

plot models for analyzing overall width, width offset, and ratio skew. After the string data were collected using the fluorometer, the weather data were sorted from the text files generated via the weather station and the Python script. Weather data for the minute before, minute during, and minute directly after each test run were manually sorted from the text files and imported into Microsoft Excel to generate wind directional components as discussed earlier in this chapter. Figure 22 shows a typical relative deposition response curve. The nozzle tested was the XP 40 at 50 psi and 10 mph.

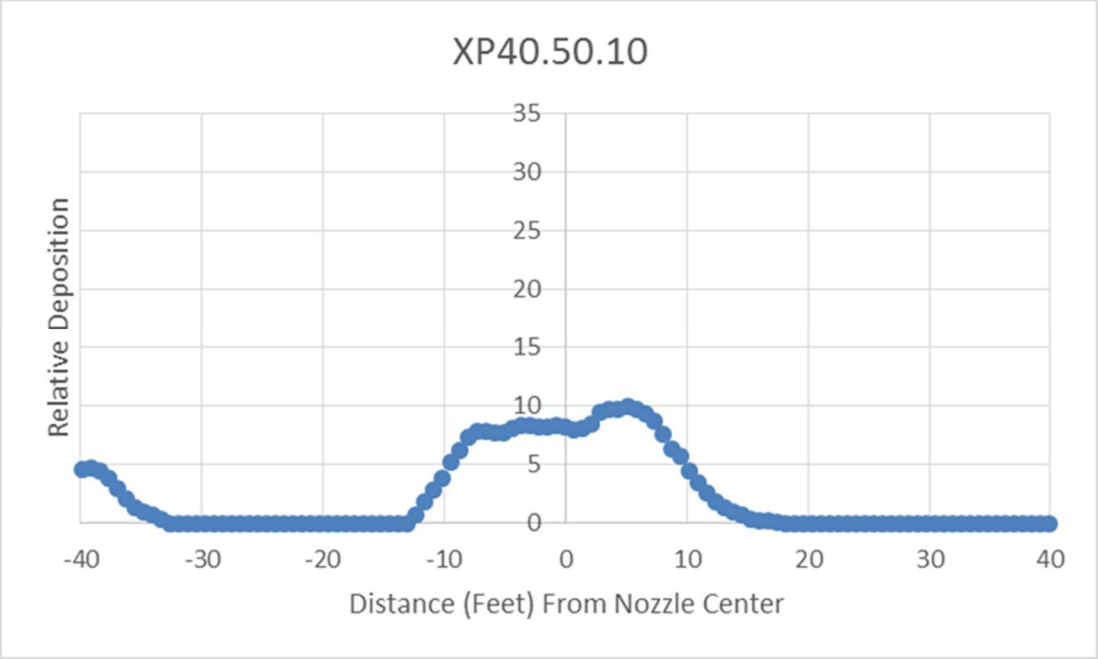

Figure 22. Typical relative deposition curve. The response near -40 feet is due to the mark on the string indicating where the data begins.

Experimental Analysis

To analyze the data in which replications were possible, including overall width, effective width, width offset, ratio skew, and area, SAS® 9.3 "Proc Mixed" (Mixed) procedure was utilized with "LSMeans." Mixed allows for unbalanced datasets as were caused by the XP40s not reaching 60 PSI (Dickey, 2007). The "by" statement in the Mixed procedure was used to analyze the high pressure nozzles and the low pressure nozzles separately. In addition, the "by" statement

was used to analyze results via nozzle model in some instances. This procedure was done to evaluate if there were any differences in how nozzles were affected by the factors of setting (indoor or outdoor), nozzle pressure, or tractor speed. In addition, a "Random" statement was used, which introduces a random error term into the model and transitions the model into a split plot design. The random error term is the replication error within the blocks, which is represented by "setting*replication" in the Mixed model. See the appendix for complete coding. Interactions were placed in the model, but if they were not significant, they were dropped from the model and the model was run again (Pasta et al, 2011). JMP® Pro 13 was used to analyze the data distributions for normality before analysis was started.

Overall Width

The width of the fluorescent swath on each string was determined by counting the number of relative data points in each run's dataset after the set was trimmed as described previously. The number was then multiplied by .72. This number is the feet per data point the fluorometer software used to calculate the net mean fluorescence. The product is the width of the fluorescent swath.

Width Offset

Width offset was defined as the distance from the midpoint of the string to the midpoint of the observed swath width. The width offset numbers were found using the trimmed datasets as previously described. The row that represented the midpoint of the string from the original 111 data points of the untrimmed data was determined. Next, the row at which the observed midpoint of the overall width of trimmed data for each test run was determined. If the midpoint occurred between rows, then the rows were averaged, e.g. 96 and 95 averaged is 95.5. The observed midpoint row was then subtracted from the midpoint row of the string. This number is positive if the offset goes north of the midpoint or negative if the offset goes south of the midpoint outdoors. Indoor offsets will be positive if the offset occurs on the tractor driver's right side from which the tractor approached the string. The row differences were then multiplied by .72. This number is the

feet per data point the fluorometer software used to calculate the net mean fluorescence. Therefore, the product is the difference, in feet, from the midpoint of the string to the midpoint of the observed swath width. Width offset results were analyzed by nozzle after an unbounded Johnson transformation was used to normalize the data. A different unbounded Johnson transformation was used for each nozzle dataset. Interaction terms were dropped for each nozzle if they were insignificant.

Effective Width

After the overall width, ratio skew, and width offset were calculated, the effective widths were calculated. The effective width was defined the portion of the swath width where the relative deposition was at 50% or above. The first step before finding the effective width was to scale the relative deposition datasets for each run to be between 0 and 100. Scaling was done by picking finding the maximum and minimum of the datasets that had been previously trimmed before to find the overall width. After the maximum and the minimum were found, the following formula was utilized to scale each number in the dataset:

$$\boldsymbol{new\ data\ point} = \frac{\mathbf{100} * (\boldsymbol{old\ data\ point} - \boldsymbol{minimum\ data\ point})}{(\boldsymbol{maximum\ data\ point} - \boldsymbol{minimum\ data\ point})}$$

Where the old data point is the data point being transformed,

the minimum data point is the minimum value from the data string,

the maximum data point is the maximum value from the data string,

and the new data point is the new scaled value.

After the datasets were scaled, the midpoint data value of the string was highlighted, and the first number closest to 50 was highlighted on each side of the midpoint. If the difference between 50 and two successive numbers were the same, but one number was above 50 and the other number was below 50, the number above 50 was selected. If two numbers of equal value occurred successfully and were both greater than or equal to 50 in value, the number that was further from the midpoint was selected. If the two numbers of equal value were less than 50, the

number that was closer to the midpoint was selected. The number of rows in Excel were counted between the two selected points, including the selected points. This number was then multiplied by .72, which is the feet per data point the fluorometer software used to calculate the net mean fluorescence. This product was defined as the effective width for that replication. In the case that the midpoint on the string was below 50 due to poor nozzle performance, the maximum value on the dataset was found, the number that came closest to 50 on either side of this data point were counted in a fashion that was the same as counting from the midpoint of the string, and then multiplied by .72. This product was defined as the effective width for the dataset. See figure 23 for a marked dataset for effective width.

48.91305	25	48.00001
58.69564	27.77777	55.99999
64.13041	34.72222	62.00004
67.39131	44.44446	70.00002
70.65216	48.61113	78.00004
71.73912	50	84
78.26087	59.72224	86.00002
84.78261	72.22221	84
88.04348	80.55555	88.00004
89.13042	100	100
100	98.61113	96.00001
100	90.27779	94.00004
100	79.16669	94.00004
97.82607	73.61111	94.00004
92.39129	73.61111	92.00003
85.86955	73.61111	90.00001
77.1739	72.22221	90.00001
70.65216	70.83335	88.00004
66.30435	66.66668	88.00004
63.04347	61.1111	80.00001
58.69564	55.55557	72.00004
55.43479	50	66.00003
51.08695	44.44446	60.00003
44.56521	36.11112	54.00002

Figure 23. Highlighted data points in Excel representing the effective width.

Areas

The area of the effective width datasets were calculated using the trapezoidal method. Two consecutive data points were averaged and then multiplied by .72, which was the width between each recorded data point as measured by the WRK of Arkansas software. This product is the area of a trapezoid. Each consecutive trapezoid was then added, calculating the approximate relative area of each dataset.

Ratio Skew

Ratio skew was defined as the percentage of the area under the curve on the left side of the swath's actual width divided by the percentage of area under the curve from the swath's right side according to the following equation:

$$\textbf{Ratio Skew} = \frac{\%\ \textbf{Area under curve left of the string midpoint}}{\%\ \textbf{Area under the curve right of the string midpoint}}$$

The same trapezoidal rule that was used to calculate the areas were used for ratio skew. However, the left side area and the right side area were calculated independently. For the left side of the data, the consecutive data points used for the trapezoids were added up from the left side to the middle, consecutively. For the right side of the data, the consecutive data points used for the trapezoids were added up from the right side to the middle. This way, the effect of the concavity of the curves that the area is being calculated from would be approximately the same for both the left side and the right side. The left and the right side were then added together to get the total area. The left side area and the right side areas were then divided by the total area to find the left area percentage and the right area percentage, and then these numbers were divided to find the ratio skew of each run's relative deposition dataset. Datasets were able to be analyzed by nozzle model and by nozzle type (high or low pressure) after using unbounded Johnson transformations. The data was then statistically analyzed and insignificant interactions were dropped from the models.

Simulated Swath Overlapping

A method was developed to simulate a relative deposition pattern with overlapping swaths using the three replications per test unit. The swaths were overlapped where the swaths were as close to 50% of the maximum as possible. The distance between swath overlapping is the effective swath width. A test unit is the particular nozzle model, location (inside or outside), pressure, and tractor speed tested. Using Microsoft Excel, datasets for the three replications of each test unit were aligned directly next to each other, with the midpoints of the strings of each dataset directly aligned. The datasets that were used were the scaled datasets used for the effective width calculations. The third replication was aligned to the left, the middle replication was kept in the middle, and first replication was on the right side. The average number of rows that was counted for each test unit was found when the effective widths were being calculated. The average number of rows was rounded down to nearest whole number of rows and divided by two. If this number of rows was even, it was rounded down to the nearest odd number of rows, and divided by two. This quotient was rounded down to the nearest whole number, and this number was the number of Excel rows that were highlighted from both sides of the middle data point of the string dataset for all replications. The average number of rows was rounded down to an odd number so the same number of rows could be highlighted on each side of the midpoint. The midpoints were highlighted a different color from the other highlights. The middle replication was then completely reversed to simulate a tractor (or another vehicle with an attached sprayer) turning around and driving in the opposite direction directly overlapping 50% of the spray swath with the first spray swath. The left and right datasets were not reversed. The wind data listed in the "Findings" section of this thesis for the middle replication was also reversed. After the middle replication was reversed, the last highlighted data point of the right (first) replication was aligned with the first highlighted data point of the middle (second) replication. The opposite was done with the left (third) replication. The first highlight data point of the left replication was aligned with the last highlighted data point of the middle replication. Next, the

sum across all data points (up to three data points for some datasets, or just a single or two data points) perpendicular to the length of the string was found. These sums across all three data points (or one or two data points) for the entire combined length of the three swaths represents the simulated overlap swath. Figures 24 through 27 highlight the process of swath overlapping.

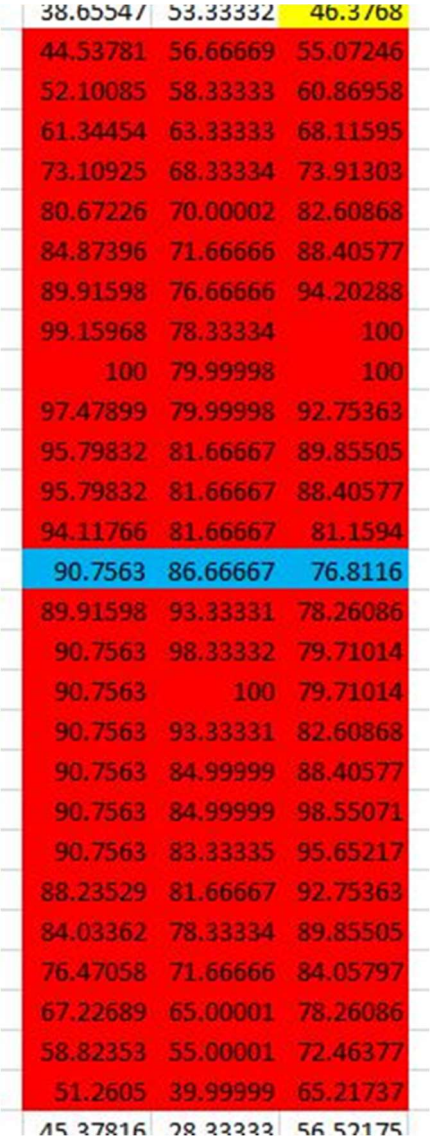

38.65547	53.33332	46.3768
44.53781	56.66669	55.07246
52.10085	58.33333	60.86958
61.34454	63.33333	68.11595
73.10925	68.33334	73.91303
80.67226	70.00002	82.60868
84.87396	71.66666	88.40577
89.91598	76.66666	94.20288
99.15968	78.33334	100
100	79.99998	100
97.47899	79.99998	92.75363
95.79832	81.66667	89.85505
95.79832	81.66667	88.40577
94.11766	81.66667	81.1594
90.7563	86.66667	76.8116
89.91598	93.33331	78.26086
90.7563	98.33332	79.71014
90.7563	100	79.71014
90.7563	93.33331	82.60868
90.7563	84.99999	88.40577
90.7563	84.99999	98.55071
90.7563	83.33335	95.65217
88.23529	81.66667	92.75363
84.03362	78.33334	89.85505
76.47058	71.66666	84.05797
67.22689	65.00001	78.26086
58.82353	55.00001	72.46377
51.2605	39.99999	65.21737
45.37816	28.33333	56.52175

Figure 24. Highlighted effective widths.

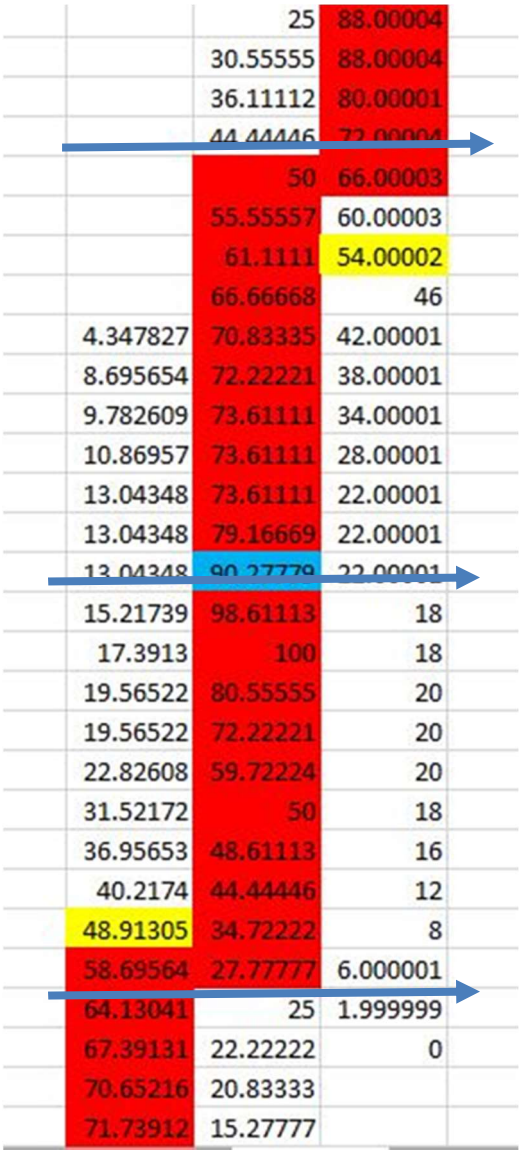

	25	88.00004
	30.55555	88.00004
	36.11112	80.00001
	44.44446	72.00004
	50	66.00003
	55.55557	60.00003
	61.1111	54.00002
	66.66668	46
4.347827	70.83335	42.00001
8.695654	72.22221	38.00001
9.782609	73.61111	34.00001
10.86957	73.61111	28.00001
13.04348	73.61111	22.00001
13.04348	79.16669	22.00001
13.04348	90.27779	22.00001
15.21739	98.61113	18
17.3913	100	18
19.56522	80.55555	20
19.56522	72.22221	20
22.82608	59.72224	20
31.52172	50	18
36.95653	48.61113	16
40.2174	44.44446	12
48.91305	34.72222	8
58.69564	27.77777	6.000001
64.13041	25	1.999999
67.39131	22.22222	0
70.65216	20.83333	
71.73912	15.27777	

Once the left and right passes were positioned, these three rows were summed across to create a new row for the entire overlapped simulated swath (not shown). Distance from center goes negative towards the top of the page, therefore the left dataset becomes the pass on the right side and vice versa.

Figure 25. Simulated Overlapping.

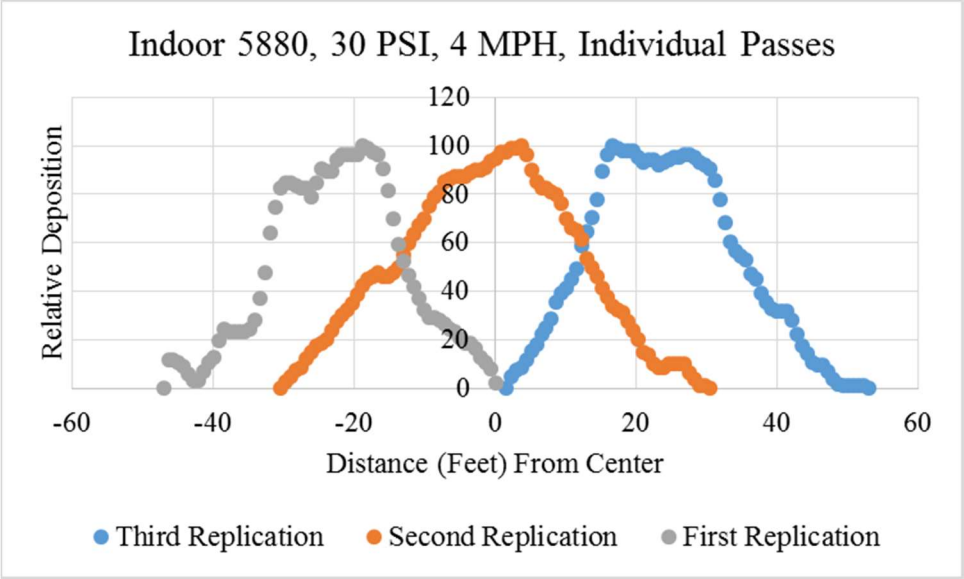

Figure 26. Individual passes.

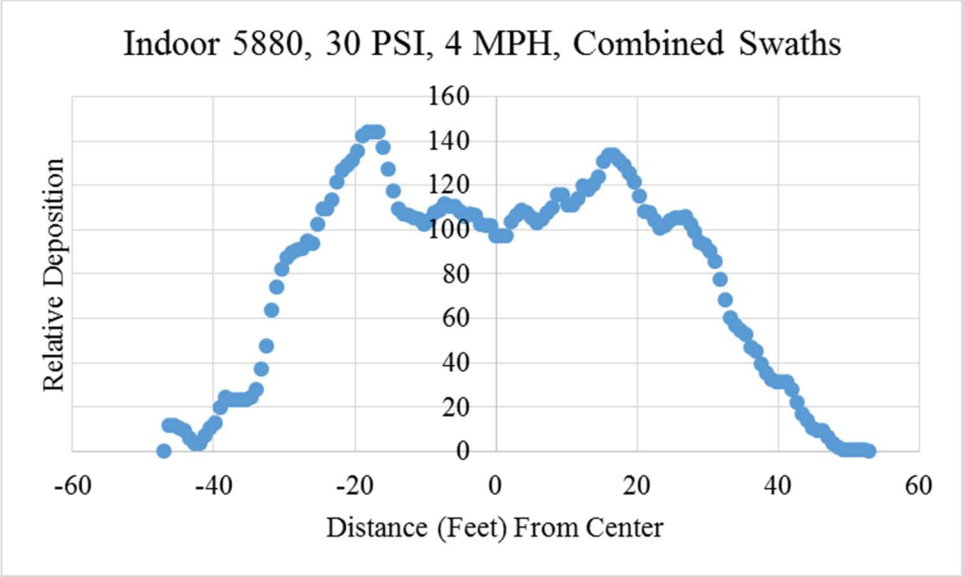

Figure 27. Combined swath from three swaths overlapping at the 50% deposition point.

Coefficient of Variation and Christiansen's Uniformity Coefficient

After the effective widths were calculated and simulated overlapped datasets were created, a coefficient of variation (CV) and Christiansen's Uniformity Coefficient (CU) were calculated for each test unit. The CV and the CU were calculated for the middle portion of the overlapped pass between where the 50% data point of the middle pass hits the 50% data points of

the left and right passes. Coefficient of Variation (CV) was calculated using the population standard deviation and average functions in Microsoft Excel. The standard deviation was divided by the average for each test unit's middle section of the simulated overlap swath. Christiansen's Uniformity Coefficient was calculated using the following formula:

$$\boldsymbol{CU = 1 - \frac{\sum_{i=1}|F_i - \overline{F}|}{\sum_{i=1}^{n} F_i}}$$

Where CU is Christiansen's Uniformity Coefficient,

n is the number of relative fluorescent data points,

F_i is the relative fluorescence (representing relative deposition) of the *i*th data point,

And $\overline{F}$ is the arithmetic average relative fluorescence (deposition) of all data points.

There is only one measure of CV and CU per test unit (no replications) because all three replications were used to generate as single simulated overlapped swath. Both CV and CU are decimal numbers ranging from 0 to 1. 1 represents a smooth curve for CU and 0 represents a smooth curve for CV.

CHAPTER IV

FINDINGS

General Test Findings

The roller pump could not generate 60 PSI for the TeeJet XP 40 nozzle. Therefore, the runs that were supposed to be 60 PSI were run at 50 PSI. These runs increased the number of replications of 50 PSI for the XP 40. Moreover, one 50 PSI, 6 MPH and one 50 PSI, 10 MPH indoor run for the XP 40 were dropped from the analysis due to inconsistent pressures. These were the only runs that were deleted, as the pressure issue was corrected for the other runs. During testing, it was observed that the platform would move a couple inches from the forces of the tractor driving across it. A couple inches of movement in the north to south or east to west direction could be observed approximately every 20 runs. After the boards had moved two inches during testing, the boards were moved back to ensure consistent testing and to allow the tractor operator to safely maneuver the tractor across the ramp.

During the third outdoor run of the Boom TD nozzle, the nozzle fell off of the back of the sprayer due to a rupture in the solenoid. This breakdown was after the last Boom TD run failed due to a rupture in a connecting pipe. After these setbacks, it was decided to end testing of the Boom TD and resume testing on the other nozzles after the solenoid of the same model was

replaced. The Boom TD was taken out of testing to ensure completion of the runs without any further material failures. The Boom TD was heaviest of the testing nozzles, and it was evident that the equipment had to be modified if it was going to not malfunction due to testing the Boom TD.

Mud began to accumulate in the arena due to the amount of water used for the experiment. However, the mud did not seem to slow the tractor down or hinder the experiment in any way but was a minor annoyance. Some mud or dirt splashed on the test string either during tractor runs over the top or when an assistant reeled in the string after a run. However, the foreign material on the string appeared negligible, and fluorometer readings did not seem to be changed.

Most of the data points were recorded successfully for the weather. However, for outdoor run number 31, which was a KLC 36 tested at 20 psi and four mph, only two minutes of weather data was recorded. The minute before the run and the minute during the run were recorded. The weather station shut down prematurely due to the laptop going to sleep. Data was checked quickly after it was noticed that the laptop was asleep, but it was not noticed that only two minutes of data for the run were recorded. In addition, a few seconds of data points were lost for many runs when the data was not recorded for wind direction, and was instead recorded as "-1." These errors appeared to get worse the longer the weather station was outside. However, the majority of the seconds of data were still recorded. In the final file of weather data, which recorded for one hour and five minutes, 3316 data points were recorded. Of these data points, 777 were "bad" data points, meaning a "-1" was recorded. Therefore, roughly 75% of the weather data was still usable accounting for .65 usable recordings per second. The reason for why missing data points occurred was not investigated, as the missing data points were not noticed until after outdoor testing was completed. The weather station recorded values at 1 hertz.

All analysis was completed using SAS® 9.4 software. Coding and transformation functions are in the appendices. All analysis was conducted using a significance level (alpha value) of 0.5.

Effective Width

Effective width data were analyzed by sorting the data by nozzle model. Data normalization was achieved for most of the nozzle data by transforming the effective width data using an unbounded Johnson distribution. Only the 5880 exhibited a normal distribution without transformation, with a Shaprio-Wilk W test p-value of .44. The remaining nozzle datasets were transformed using JMP® and the Shapiro-Wilk W test p-values were found to be .33, .14, .19, .20, .08, and .35 for the KLC 18, XP 25, XP 40, and XT 024. The data was then transferred to SAS® and examined using Mixed. Interactions were dropped if they were found to be insignificant.

Effective width is the width at which the tractor will be spacing passes to effectively cover the targeted area. Therefore, it is important to know what factors play a significant role in changing the effective width. Two nozzles exhibited a three way setting by pressure by speed interaction. The KLC 18 and the XP 25 had this three way interaction. Pressure, speed, and wind are affecting the mean values of effective widths differently at different values of each other. This makes it very challenging to accurately predict what will happen at different levels of the tested factors for these nozzles. The 5880 and the Hamilton had setting by pressure significant interactions. This is expected, because pressure is theoretically a direct factor in changing pattern widths, and changing the setting from outside to inside reduces wind, which reduces drift, another factor in the effective width of a nozzle. Speed was a significant interaction for the 5880, KLC 36, XP 40, and XT 024. Speed reduces application rate going to the ground, so it is not surprising the speed was a significant effect for these nozzles. Pressure was a significant effect for the KLC 36, XP 40, and XT 024. Again, this effect is not surprising because pressure is a factor that changes application rate. Setting was significant effect for the KLC 36 and the XP 40, which is not ideal. This effect means that changing the location from a non-windy environment to a windy one changes the effective width. However, the extent of the effect may be able to be managed if

the wind conditions are known and spraying practices are modified. Parameters for effective width are shown in table 2.

Table 3 shows a comparison between measured effective width and advertised width. These least squares means were calculated without speed to be consistent with manufacturers. Least squares means in the appendix do use speed as a factor, however. It can be noticed that all the effective widths that were measured were shorter than advertised lengths. These differences mean that manufacturers most likely are not using effective width as their definition of what a width is. Nozzle users need to be aware of the difference, and be aware that the effective width may be much lower than the advertised widths in many cases.

Table 2. F values including the numerator and denominator degrees of freedom (NDF, DDF) and P values of the dependent variables for effective width. Italics indicate significant effects at alpha = .05.

Effective Width Parameter Effects

Parameter		Nozzle 5880	KLC 18	KLC 36	Ham	XP 25	XP 40	XT 024
Setting	F (NDF, DDF)	8.1 (1, 4)	0.22 (1, 4)	20 (1, 4)	15 (1, 4)	4.6 (1, 4)	10 (1, 9.37)	0.63 (1, 4)
	P Value	*0.05*	0.66	*0.01*	*0.02*	0.10	*0.01*	0.47
Pressure	F (NDF, DDF)	3.0 (2, 42)	2.3 (2, 32)	4.8 (2, 44)	0.98 (2, 42)	0.09 (2, 32)	4.0 (1, 47)	3.5 (2, 44)
	P Value	0.06	0.11	*0.01*	0.38	0.92	*0.05*	*0.04*
Speed	F (NDF, DDF)	6.1 (2, 42)	8.0 (2, 32)	15 (2, 44)	2.6 (2, 42)	2.3 (2, 32)	5.2 (2, 39.7)	5.9 (2, 44)
	P Value	*<.01*	*<.01*	*<.01*	0.08	0.12	*<.01*	*<.01*
Setting x Speed	F (NDF, DDF)		1.1 (2, 32)			0.13 (2, 32)		
	P Value		0.35			0.88		
Setting x Pressure	F (NDF, DDF)	4.8 (2, 42)	0.36 (2, 32)		3.4 (2, 42)	2.3 (2, 32)		
	P Value	*0.01*	0.70		*0.04*	0.11		
Pressure x Speed	F (NDF, DDF)		2.8 (4, 32)			0.78 (4, 32)		
	P Value		*0.05*			0.55		
Setting x Pressure x Speed	F (NDF, DDF)		4.3 (4, 32)			3.0 (4, 32)		
	P Value		*<.01*			*0.03*		

Table 3. Comparison of effective width means and advertised widths.

Effective Width Least Squares Means and Advertised Widths

Nozzle	Pressure (PSI)	Advertized Width (ft)	Indoor Width (ft)	Outdoor Width (ft)
5880	20	47	17	19
	30	50	22	17
	40	52	23	20
KLC 18	20	20	13	13
	30	21	14	14
	40	22	14	13
KLC 36	20	22	17	15
	30	24	19	16
	40	26	19	17
XP 25	40	29	17	17
	50	30	19	17
	60	32	19	16
XP 40	40	31	21	18
	50	32	21	20
	60	35	NOT TESTED	
Ham	40	54	16	16
	50	56	18	14
	60	58	19	15
XT 024	40	32*	20	18
	50	32*	18	18
	60	32*	21	19

*Listed at 48 inches height. Tests were conducted at 36 inches height.

Overall Width

Width is what many consumers look at when considering which nozzles to use. Therefore, determining which dependent variables affect the width for individual nozzles is very important for nozzle users.

To normalize the data, unbounded Johnson transformations were used for each nozzle dataset. A p-value for the Shapiro-Wilk W test of .4999 for the 5880, .8057 for the Hamilton, .6389 for the KLC 18, .7717 for the KLC 36, .5283 for XP 25, .9687 for the XP 40, and .9688 for

the XT 024 were all over the alpha value of .05. These p-values indicate the null hypotheses, that the datasets were from the normal distribution, were not rejected. As each nozzle was analyzed individually, interaction terms were dropped if they were found be insignificant at the 95% confidence level.

According to the statistical analysis shown in Table 4, only three nozzles experienced significant effects. The TeeJet BoomJet 5880 nozzle experienced a significant setting by speed interaction. The TeeJet BoomJet XP 25 had a significant setting by pressure interaction. Finally, the Hypro Pentair XT 024 had a significant setting effect. All three of these significant effects have changing the testing location from indoors to outdoors either as a factor by itself as a significant effect or with another variable as an interaction. The least squares means shown in Table 5 indicates that both the 5880, XT 024, and XP 25 all increased for two and out of three pressures when moving from indoors to outdoors. The table also shows that the TeeJet FieldJet KLC 18 and KLC 36 were the only nozzles that met or exceeded the manufacturer's advertised width rating both indoors and outdoors for all pressures compared to the least squares means estimate. These varying results indicates that the manufacturers' methods for measuring width is inconsistent and a standard method for the measurement of boomless nozzle swath width would be beneficial to consumers. However, all nozzles' advertised widths were within the statistical 95% confidence interval with the exception of the Hamilton, which had a smaller advertised width. Finally, 16 out of 20 pressure and nozzle test combinations indicated a swath width increase from moving indoors to outdoors. This increase is probably due to the wind that occurred outdoors spreading the droplets as they left the nozzle across a wider area than if no wind were present. However, a wider swath due to wind may not be a good thing, because the swath may be more inconsistent in deposition across its width, contributing to streaking in pastures or fields.

Table 4. F values including the numerator and denominator degrees of freedom (NDF, DDF) and P values of the dependent variables for width. Italics indicate significant effects at alpha = .05.

Overall Width Parameter Effects

		Nozzle						
Parameter		5880	KLC 18	KLC 36	Ham	XP 25	XP 40	XT 024
Setting	F (NDF, DDF)	9.9 (1, 4)	4.4 (1, 4)	0.30 (1, 4)	1.3 (1, 4)	0.88 (1, 4)	0.04 (1, 8.45)	13 (1, 4)
	P Value	*0.03*	0.10	0.61	0.32	0.88	0.85	*0.02*
Pressure	F (NDF, DDF)	0.86 (2, 42)	0.30 (2, 44)	1.3 (2, 44)	0.09 (2, 44)	0.41 (2, 42)	0.43 (1, 46.2)	3.1 (2, 44)
	P Value	0.43	0.75	0.28	0.91	0.41	0.52	0.06
Speed	F (NDF, DDF)	6.0 (2, 42)	3.0 (2, 44)	1.2 (2, 44)	3.2 (2, 44)	0.24 (2, 42)	0.76 (2, 37.9)	0.47 (2, 44)
	P Value	*<.01*	0.06	0.30	*0.05*	0.79	0.47	0.63
Setting x Speed	F (NDF, DDF)	5.0 (2, 42)						
	P Value	*0.01*						
Setting x Pressure	F (NDF, DDF)					4.1 (2, 42)		
	P Value					*0.02*		

Table 5. Comparison of the Least Squares Means and 95% confidence intervals against the advertised widths of each nozzle to the nearest foot. Pink indicates values that are lower than advertised, blue indicates values that are higher than advertised, and green indicates values that are the same as advertised.

Overall Width Least Squares Means Estimates and Advertised Widths

Nozzle	Pressure (PSI)	Advertized Width (ft)	Indoor Width (ft)	Indoor 95% CI (ft)	Outdoor Width (ft)	Outdoor 95% CI (ft)
	20	47	46	42-50	53	48-60
5880	30	50	47	43-52	59	52-67
	40	52	49	45-55	49	45-55
	20	20	27	23-34	32	26-41
KLC 18	30	21	27	23-34	34	28-45
	40	22	30	25-38	34	27-44
	20	22	29	26-32	32	29-37
KLC 36	30	24	32	29-38	31	28-36
	40	26	33	30-40	33	30-39
	40	29	26	24-31	35	28-53
XP 25	50	30	28	25-34	29	25-37
	60	32	29	25-37	27	24-33
	40	31	33	28-41	32	28-40
XP 40	50	32	31	28-35	32	29-36
	60	35	NOT TESTED			
	40	54	34	29-42	43	35-56
Ham	50	56	34	29-41	41	33-53
	60	58	41	33-52	36	30-45
	40	32*	29	26-32	29	27-33
XT 024	50	32*	30	27-34	36	31-43
	60	32*	31	28-36	36	32-44

*Listed at 48 inches height. Tests were conducted at 36 inches height.

Area

Area data were analyzed by breaking the data down by nozzle model. Data normalization was achieved for some of the nozzle data by transforming the area data using an unbounded Johnson distribution. The 5880, Hamilton, and KLC 36 distributions were found to be normal

without transformations, with Shapiro-Wilk W test p-values of .73, .56, and .79, respectively. The other datasets were transformed using JMP® and the Shapiro-Wilk W test p-values were found to be .37, .90, .87, and .60 for the KLC 18, XP 25, XP 40, and XT 024. The data were then transferred to SAS® and examined using Mixed. Interactions were dropped if they were found to be insignificant.

Area of the relative deposition curves indicates the relative amount of spray that was deposited across the swath width. If the area changes, the application rate has theoretically changed. Results in this section need to be analyzed with caution, however. This is because area is dependent on the relative amount of fluorescence that was measured on each data point going across the string by the fluorometer. Slight differences in dye and water mixtures can significantly impact area measurements. This was accounted for by scaling the data between 0 and 100. However, fluorescence is also dependent on droplet size, which changes with pressure. (Whitney and Roth). It is unknown how much droplet sizes changed with the nozzles tested as the pressure was varied. Dependent variable effects can be seen in table 6. Neither the XP 25 nor the XP 40 exhibited significant results, which is surprising because pressure and speed both change flow rate. The 5880 and KLC 36 exhibited a significant setting by speed interaction. This indicates that wind and speed may be playing a factor in reducing application rates. Both the KLC 18 and the Hamilton exhibited significant setting (location) effects. Once again, the wind is may be reducing flow rates due to drift. Finally, the XT 024 exhibited a setting by pressure interaction. This interaction is not surprising, as pressure changes flow rate and changing the location of the nozzle from inside to outside can lead to drift.

Table 6. F values including the numerator and denominator degrees of freedom (NDF, DDF) and P values of the dependent variables for area. Italics indicate significant effects at alpha = .05.

Area Parameter Effects

		Nozzle						
Parameter		5880	KLC 18	KLC 36	Ham	XP 25	XP 40	XT 024
Setting	F (NDF, DDF)	37 (1, 4)	53 (1, 4)	2.2 (1, 4)	32 (1, 4)	0.24 (1, 4)	3.2 (1, 10.2)	1.9 (1, 4)
	P Value	*<.01*	*<.01*	0.21	*<.01*	0.65	0.10	0.24
Pressure	F (NDF, DDF)	0.06 (2, 42)	0.18 (2, 44)	2.8 (2, 42)	0.55 (2, 44)	1.7 (2, 44)	0.86 (1, 46.9)	0.90 (2, 42)
	P Value	0.06	0.84	0.07	0.58	0.19	0.36	0.41
Speed	F (NDF, DDF)	2.2 (2, 42)	2.4 (2, 44)	1.4 (2, 42)	.16 (2, 44)	0.43 (2, 44)	0.18 (2, 40.1)	0.04 (2, 42)
	P Value	0.12	0.10	0.25	0.86	0.65	0.84	0.96
Setting x Speed	F (NDF, DDF)	9.2 (2, 42)		5.2 (2, 42)				
	P Value	*<.01*		*0.01*				
Setting x Pressure	F (NDF, DDF)							4.6 (2, 42)
	P Value							*0.02*

Width Offset

Width offset measures how much the midpoint of the swath width changes from the midpoint of the string. Width offset results were analyzed by nozzle after an unbounded Johnson transformation was used to normalize the data. A p-value for the Shapiro-Wilk W test of .2644 for the 5880, .0868 for the Hamilton, .8205 for the KLC 18, .8349 for the KLC 36, .6282 for XP 25, .7655 for the XP 40, and .8835 for the XT 024 all are over the alpha value of .05, indicating that the null hypothesis that the datasets were from the normal distribution were not rejected. A different unbounded Johnson transformation was used for each nozzle dataset. Table 7 shows that there were no significant effects on width offset for the high pressure nozzles. The low pressure nozzles had a setting significant effect as well as a third-order pressure by speed by nozzle significant interaction. These effects may be due to the overall lower pressures of the low pressure nozzles compared to the high pressure nozzles. Low pressure nozzles were tested at 20, 30, and 40 psi compared to 40, 50, and 60 psi for the high pressure nozzles. The lower pressure may have allowed the wind to push the swath and change the midpoint. When wind offset was further broken down by nozzle (Table 8), there were only two significant effects. These were both setting on the 5880 and the KLC 18. Changing the pressure or the tractor speed was not a

significant factor for any nozzle. This result was expected, as nozzles are not designed to change the midpoint of swath when pressure changes. In addition, none of the other nozzles besides the 5880 and KLC 18 were affected by changing the location of the nozzle from outdoors to indoors. Another factor that may affect width offset is droplet size. Droplet size was not measured for this experiment, it may be useful to relate droplet size to width offset, coefficient of variation, or other independent variables.

Table 7. F values including the numerator and denominator degrees of freedom (NDF, DDF) and P values of the dependent variables for width offset by nozzle type. Italics indicate significant effects at alpha = .05.

Width Offset Parameter Effects by Type

		Nozzle Type	
Parameter		High Pressure	Low Pressure
Nozzle	F (NDF, DDF)	1.2 (3, 202)	1.5 (2, 124)
	P Value	0.31	0.23
Setting	F (NDF, DDF)	0.00 (1, 5.49)	41 (1, 4)
	P Value	0.99	*<.01*
Pressure	F (NDF, DDF)	1.5 (2, 201)	2.7 (2, 124)
	P Value	0.22	0.07
Speed	F (NDF, DDF)	0.04 (2, 199)	0.11 (2, 124)
	P Value	0.96	0.89
Pressure x	F (NDF, DDF)		2.1 (8, 124)
Speed x Nozzle	P Value		*0.04*

Table 8. F values including the numerator and denominator degrees of freedom (NDF, DDF) and P values of the dependent variables for width offset by specific nozzle. Italics indicate significant effects at alpha = .05.

Width Offset Parameter Effects by Nozzle

		Nozzle Type						
Parameter		5880	KLC 18	KLC 36	Ham	XP 25	XP 40	XT 024
Setting	F (NDF, DDF)	10. (1, 4)	98 (1, 4)	0.17 (1, 4)	1.1 (1, 4)	0.63 (1, 4)	0.06 (1, 3.24)	1.1 (1, 4)
	P Value	*0.03*	*<.01*	0.70	0.36	0.47	0.82	0.35
Pressure	F (NDF, DDF)	1.9 (2, 44)	2.9 (2, 44)	2.0 (2, 44)	0.88 (2, 44)	2.2 (2, 44)	0.27 (1, 46.6)	1.3 (2, 44)
	P Value	0.17	0.07	0.15	0.42	0.12	0.61	0.28
Speed	F (NDF, DDF)	0.09 (2, 44)	0.49 (2, 44)	1.9 (2, 44)	0.10 (2, 44)	0.04 (2, 44)	0.03 (2, 35.3)	0.03 (2, 44)
	P Value	0.92	0.61	0.16	0.91	0.96	0.97	0.97

Ratio Skew

Ratio skew indicates how uneven the application amount is across the swath. This unevenness can contribute to streaking during nozzle operation. The data was transformed using JMP® and the Shapiro-Wilk W test p-values by type were found to be .1597 and .0753 for low and high, both satisfactory. The p-values for each individual nozzle were found to be .4522, .0611, .8134, .4326, .8554, .7224, and .8696 for the 5880, Hamilton, KLC 18, KLC 36, XP 25, XP 40, and XT 024, respectively. The data was then statistically analyzed and insignificant interactions were dropped from the models. Table 9 shows the effects on ratio skew by type and table 10 shows the effects by nozzle. The high pressure nozzles showed significant interactions of setting by speed and pressure by speed. The low pressure nozzles had a setting by nozzle significant interaction. However, when the experiment is broken down by nozzle, the only significant effect is setting on the KLC 18. Other significant interactions may not be present due to sample size being reduced when the nozzles are analyzed individually. The pressure by speed interaction with the high pressure nozzles is concerning because changing the pressure or tractor speed ideally should not change the evenness of the relative amount of deposition applied across the swath width. The pressure by speed interaction may have been caused by lack of quality

control, nozzle wear, or imprecise nozzle setup. A setting by nozzle interaction for both nozzle types is not unexpected, as outdoor wind is expected to affect various nozzles differently.

Table 9. F values including the numerator and denominator degrees of freedom (NDF, DDF) and P values of the dependent variables for ratio skew by nozzle type. Italics indicate significant effects at alpha = .05.

Ratio Skew Parameter Effects by Type

		Nozzle Type	
Parameter		High	Low
Nozzle	F (NDF, DDF)	3.5 (3, 196)	1.4 (2, 148)
	P Value	*0.02*	0.25
Setting	F (NDF, DDF)	0.17 (1, 8.29)	1.7 (1, 4)
	P Value	0.69	0.26
Pressure	F (NDF, DDF)	1.7 (2, 196)	0.55 (2, 148)
	P Value	0.18	0.58
Speed	F (NDF, DDF)	0.99 (2, 193)	0.31 (2, 148)
	P Value	0.37	0.73
Setting x Nozzle	F (NDF, DDF)	4.8 (3, 194)	5.7 (2, 148)
	P Value	*<.01*	*<.01*
Pressure x Speed	F (NDF, DDF)	2.9 (4, 192)	
	P Value	*0.03*	

Table 10. F values including the numerator and denominator degrees of freedom (NDF, DDF) and P values of the dependent variables for ratio skew by specific nozzle. Italics indicate significant effects at alpha = .05.

Ratio Skew Parameter Effects by Nozzle

		Nozzle Type						
Parameter		5880	KLC 18	KLC 36	Ham	XP 25	XP 40	XT 024
Setting	F (NDF, DDF)	0.04 (1, 4)	15 (1, 4)	0.09 (1, 4)	4.0 (1, 4)	0.38 (1, 4)	4.7 (1, 8.13)	1.1 (1, 4)
	P Value	0.85	*0.02*	0.78	0.12	0.57	0.06	0.35
Pressure	F (NDF, DDF)	2.0 (2, 44)	0.78 (2, 44)	2.0 (2, 44)	2.0 (2, 44)	1.7 (2, 44)	0.13 (1, 46.9)	1.5 (2, 44)
	P Value	0.14	0.47	0.15	0.15	0.20	0.72	0.23
Speed	F (NDF, DDF)	0.26 (2, 44)	0.01 (2, 44)	0.44 (2, 44)	0.34 (2, 44)	0.11 (2, 44)	0.11 (2, 40)	1.0 (2, 44)
	P Value	0.77	0.99	0.65	0.71	0.90	0.90	0.36

Coefficient of Variation and Christiansen's Uniformity Coefficient

Both the CV and the CU are decimal numbers (that can be converted into percentages). A higher CU and a lower CV are more desirable, indicative of a smoother swath pattern. Table 11 shows the CV and CU values that were obtained for this study. A CU of .80 or above is considered acceptable for sprinkler systems (Regan, 1987). The nozzles in this study are similar to sprinkler systems in that both the nozzles and the sprinklers have to spray in wide patterns compared to traditional boomed nozzles. Because of this similarity, .80 will be used in this paper as well. Most of the nozzles in this study were generally above .80 for most test units indoors. The XP nozzles and the KLC 36 nozzle exhibited CUs below .80 many times during outdoor testing, however. The KLC 36 yielded a CU .34 and a .32 with 40 psi and four mph and six mph, respectively. These pressures are both at the higher end of the pressure range for this nozzle, causing smaller droplets, possibly leading to drift. Overall for the nozzles, a trend of lower outside CU values was observed compared to inside. Also, relating CU to pressure and speed were investigated. However, more replications are needs to confirm a relationship.

A simple comparison was made to compare CV and CU. CV and CU were graphed against each other for various nozzles, shown in figures 28 through 31. A negative linear relationship was evident, with a coefficient of determination of .98 or above when there were at least nine data points. When there were only six data points, the coefficient of determination dropped to .89. In general, either number should be efficient to analyze these nozzles.

Table 11. Coefficient of Variation and Christiansen's Uniformity Coefficient

Press.Speed (PSI.MPH)	Para-meter	5880		KLC 18		KLC 36		Ham		XP 25		XP 40		XT 024	
		In.	Out.	**In.**	Out.	**In.**	Out.	**In.**	Out.	**In.**	Out.	**In.**	Out.	**In.**	Out.
20.4	CU	**0.92**	0.96	**0.82**	0.86	**0.91**	0.90	Outside Tested Range							
	CV	***0.10***	*0.05*	***0.21***	*0.16*	***0.12***	*0.12*								
20.6	CU	**0.92**	0.79	**0.94**	0.93	**0.91**	0.57								
	CV	***0.10***	*0.25*	***0.07***	*0.09*	***0.10***	*0.46*								
20.8	CU	**0.90**	0.89	**0.90**	0.79	**0.89**	0.78								
	CV	***0.13***	*0.14*	***0.11***	*0.25*	***0.14***	*0.27*								
30.4	CU	**0.96**	0.88	**0.85**	0.82	**0.90**	0.88								
	CV	***0.04***	*0.14*	***0.17***	*0.22*	***0.11***	*0.13*								
30.6	CU	**0.89**	0.70	**0.85**	0.83	**0.90**	0.89								
	CV	***0.12***	*0.32*	***0.18***	*0.21*	***0.12***	*0.13*								
30.8	CU	**0.95**	0.89	**0.82**	0.85	**0.90**	0.76								
	CV	***0.07***	*0.11*	***0.20***	*0.16*	***0.12***	*0.28*								
40.4	CU	**0.90**	0.92	**0.78**	0.83	**0.80**	0.34								
	CV	***0.11***	*0.11*	***0.24***	*0.21*	***0.23***	*0.76*								
40.6	CU	**0.94**	0.93	**0.92**	0.87	**0.93**	0.32	**0.95**	0.48	**0.67**	0.85	**0.86**	0.88	**0.82**	0.65
	CV	***0.08***	*0.09*	***0.09***	*0.16*	***0.08***	*0.76*	***0.06***	*0.56*	***0.37***	*0.18*	***0.17***	*0.14*	***0.21***	*0.42*
40.8	CU	**0.95**	0.61	**0.88**	0.80	**0.92**	0.84	**0.95**	0.93	**0.77**	0.78	**0.77**	0.82	**0.87**	0.76
	CV	***0.06***	*0.44*	***0.13***	*0.22*	***0.10***	*0.18*	***0.06***	*0.08*	***0.28***	*0.25*	***0.25***	*0.21*	***0.19***	*0.26*
40.10	CU	Outside Tested Range						**0.89**	0.87	**0.86**	0.89	**0.81**	0.62	**0.90**	0.58
	CV							***0.13***	*0.15*	***0.17***	*0.14*	***0.23***	*0.44*	***0.15***	*0.48*
50.6	CU							**0.94**	0.77	**0.82**	0.70	**0.79**	0.71	**0.81**	0.73
	CV							***0.07***	*0.25*	***0.23***	*0.39*	***0.24***	*0.39*	***0.24***	*0.32*
50.8	CU							**0.95**	0.85	**0.89**	0.73	**0.80**	0.67	**0.87**	0.53
	CV							***0.06***	*0.16*	***0.13***	*0.37*	***0.25***	*0.39*	***0.15***	*0.63*
50.10	CU							**0.94**	0.89	**0.73**	0.89	**0.82**	0.65	**0.85**	0.69
	CV							***0.07***	*0.11*	***0.32***	*0.12*	***0.20***	*0.39*	***0.19***	*0.33*
60.6	CU							**0.92**	0.92	**0.88**	0.19	Outside Tested Range		**0.91**	0.87
	CV							***0.09***	*0.09*	***0.15***	*0.89*			***0.12***	*0.19*
60.8	CU							**0.94**	0.68	**0.82**	0.54			**0.88**	0.86
	CV							***0.08***	*0.34*	***0.22***	*0.58*			***0.14***	*0.16*
60.10	CU							**0.93**	0.80	**0.80**	0.89			**0.89**	0.82
	CV							***0.09***	*0.22*	***0.23***	*0.14*			***0.13***	*0.23*

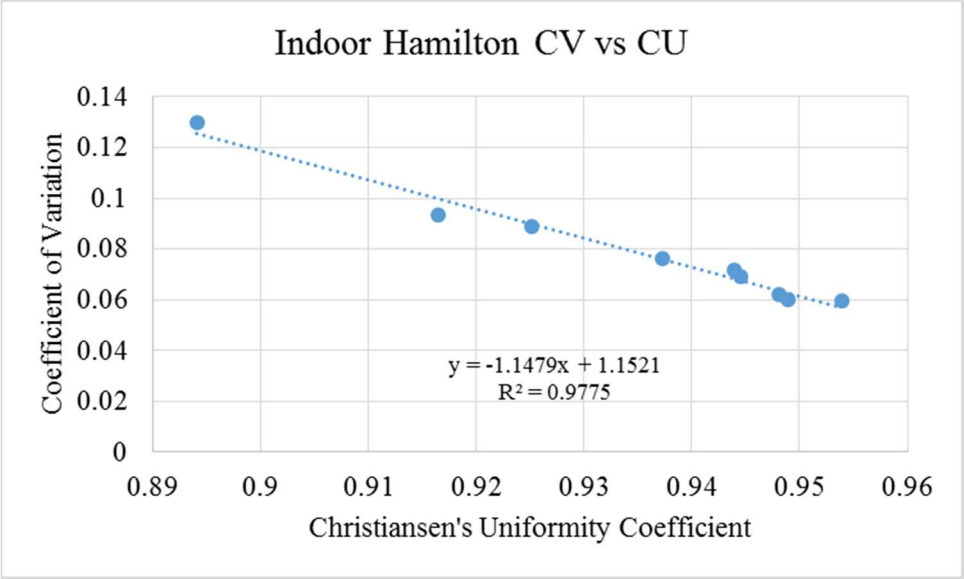

Figure 28. CV vs CU graph for indoor Hamilton.

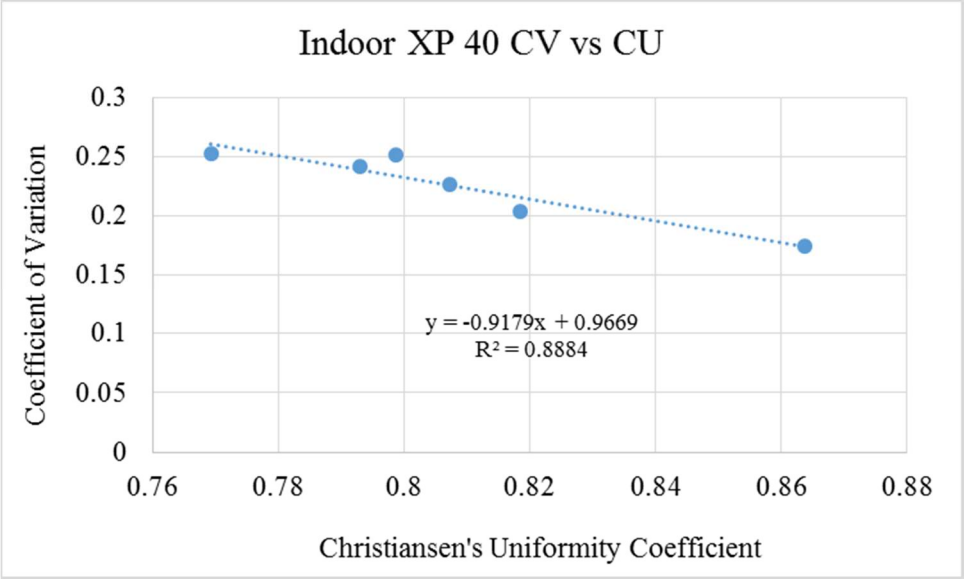

Figure 29. CV vs CU graph for indoor XP 40.

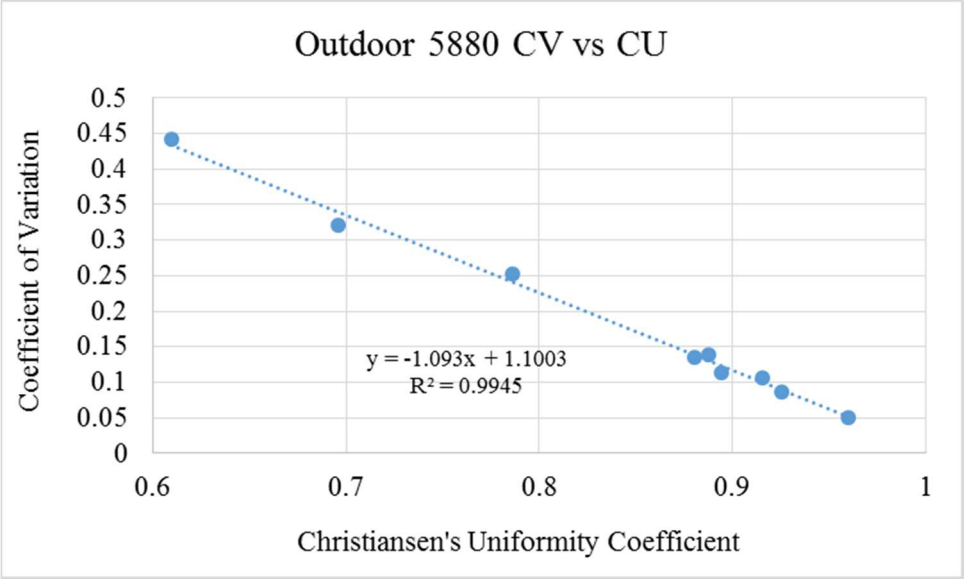

Figure 30. CV vs CU graph for outdoor 5880.

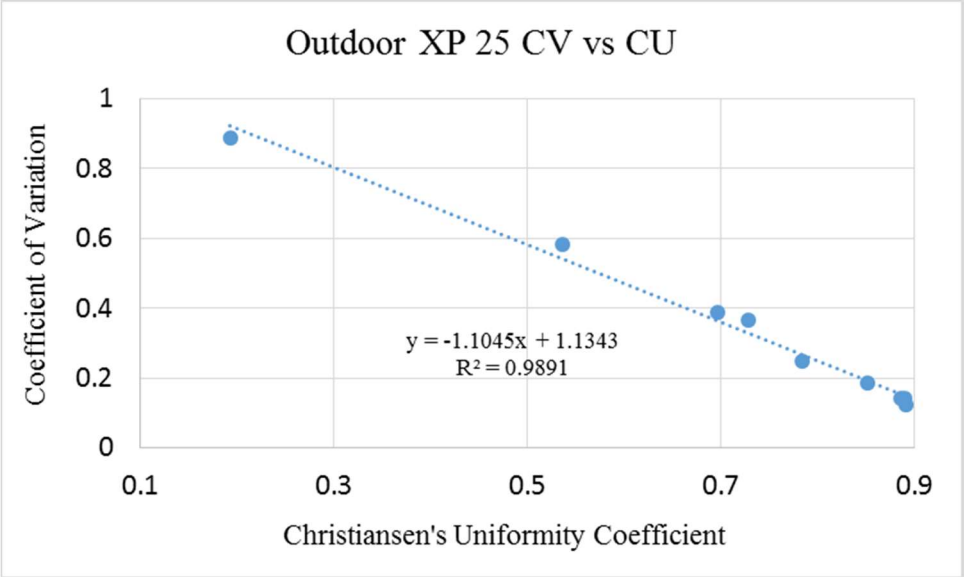

Figure 31. CV vs CU graph our outdoor XP 25.

Wind Data

Tables 12 and 13 show the wind data that was recorded during outdoor testing. This wind data can be used for picking out the higher wind conditions that the nozzles were subjected to and matching the wind data to the CV and CU data. The Hamilton wind data for 40 PSI and six MPH is matched to a .48 outdoor CU. This low value may be due to a high 9.6 MPH crosswind for the

middle replication, which comprises the bulk of the data points that are used to calculate CU. More analysis and replications to generate more CU values per test unit will be very useful to relate CU to wind conditions.

After multiple attempts to form a regression equation to relate an aspect of wind to one of the measured independent variables, the regression equation was abandoned. Different types of fits were attempted, but none worked in a convincing manner. Reasons why a regression equation may have not been possible include experimental error and too few replications. Three replications per experimental unit was the maximum amount of replications that were possible given the time allotted for this research. However, more replications would give a more robust experimental design and perhaps form a more measureable effect of wind on spray patterns. In addition, experimental error due to tractor vibrations, measurement height of the nozzle, or the software being started manually for every string may have affected measurement accuracy and precision. Recommendations for forming a useable regression equation include increasing replications, testing only a single nozzle at a single pressure and a single tractor speed, make use of a simulated wind environment (if possible), and automate the software of the fluorometer. Increasing the replications and using only a single nozzle at the same pressure and speed will ensure that the effect of random error between replications will be reduced and will also greatly simplify the experimental design. A simulated wind environment will ensure consistent winds that will be easily recordable and replicable. Automated software will reduce user error from the reaction time of the software operator.

Table 12. Wind speeds experienced during testing for low pressure nozzles.

Press. (PSI)	Rep.	5880	KLC 18	KLC 36
		Wind Speed (MPH)		
20.4	left	4.9	3.6	-0.9
	middle	*-5.6*	*-3.5*	*-3.7*
	right	4.2	3.1	4.9
20.6	left	0.0	10.2	-3.2
	middle	*2.7*	*-10.2*	*1.8*
	right	2.9	4.8	-1.5
20.8	left	6.3	6.6	2.9
	middle	*-5.5*	*-4.2*	*-3.3*
	right	3.1	5.2	1.5
30.4	left	7.2	5.2	5.7
	middle	*4.1*	*-6.5*	*-3.1*
	right	-9.9	5.0	3.5
30.6	left	-2.6	8.7	7.0
	middle	*-3.8*	*-8.4*	*-4.5*
	right	5.2	5.6	4.5
30.8	left	6.2	-1.7	-3.4
	middle	*-4.0*	*-2.3*	*-3.4*
	right	5.4	5.9	4.9
40.4	left	9.3	6.1	-3.8
	middle	*-8.1*	*-3.9*	*2.7*
	right	-8.0	3.2	-0.8
40.6	left	6.0	3.6	5.3
	middle	*1.6*	*-2.6*	*8.8*
	right	4.7	2.3	3.5
40.8	left	-2.6	6.4	-2.6
	middle	*2.7*	*5.8*	*-4.8*
	right	3.4	5.4	5.5

Table 13. Wind speeds experienced during testing for high pressure nozzles.

Press. (PSI)	Rep.	Ham	XP 25	XP 40	XT 024
		Wind Speed (MPH)			
40.6	left	-4.0	3.2	2.5	-2.1
	middle	*9.6*	*-1.4*	*-2.7*	*4.7*
	right	4.3	2.9	4.4	5.2
40.8	left	12.2	5.1	7.4	8.8
	middle	*-1.4*	*-4.3*	*-7.5*	*-5.7*
	right	-9.8	6.1	5.5	-1.3
40.10	left	11.6	8.6	11.1	-2.5
	middle	*0.2*	*-3.1*	*4.3*	*3.6*
	right	3.3	3.7	-3.4	5.2
50.6	left	6.6	-6.3	-0.3	5.0
	middle	*8.3*	*-4.4*	*8.7*	*-4.0*
	right	4.4	8.7	5.1	3.9
50.8	left	5.6	5.5	-0.5	-0.8
	middle	*-5.3*	*-4.6*	*10.9*	*-2.8*
	right	3.4	5.2	-8.7	4.9
50.10	left	7.0	8.9	3.6	-3.1
	middle	*-3.4*	*-3.3*	*8.5*	*-2.0*
	right	5.4	4.9	5.2	4.1
60.6	left	-2.3	-4.4	Outside Test Range	7.2
	middle	*-4.0*	*-2.9*		*1.6*
	right	2.5	4.3		5.2
60.8	left	2.1	7.3		-3.3
	middle	*1.8*	*5.0*		*-3.6*
	right	-6.2	-2.5		6.4
60.10	left	3.3	3.7		-6.6
	middle	*-2.8*	*-3.2*		*-3.2*
	right	7.6	5.4		-1.8

Nozzle Graphs

Nozzle relative deposition graphs shown in figures 32, 33, and 34 proved to be a useful tool to evaluate relative deposition patterns of the various nozzle models included in this study. The indoor graphs serve as a baseline of how well the nozzles can perform in ideal, minimum-wind environmental conditions. They can be compared to the outdoor graphs to determine if wind affects the spray patterns being deposited on the ground. Desirable deposition curves are those that are smooth across the entire curve. Sharp peaks and valleys may contribute to streaking in the

field. Less pronounced slopes on the curves as they increase or decrease, which leaves a more flat curve, is also desirable. The lack of steep curvature will lead to a more consistent application rate across the width of the deposition swath. The figures at the end of this section all come from the same nozzle, exhibiting vastly different results indoors and outdoors. The Hamilton, when spraying at 40 PSI and 6 MPH, yielded a CU of .95 indoors and .48 outdoors. .95 is among the highest CUs measured, and .48 is one of the lower measured in this study. The combined simulated overlap graph for the outdoor swaths shows that some ground is not even covered in what should be the overlapped area. The surface plot confirms the outdoor deposition graph, exhibiting inconsistent patterns across the three replications. The surface shows crosswinds of 4.3 to 9.6 MPH factored into nozzle deposition pattern. The indoor overlapped swath exhibits a much smoother pattern, most likely due to the absence of wind indoors. This thesis is not primarily about deposition graphs, so more graphs were not generated. However, more graph analysis may prove useful for future boomless nozzle research.

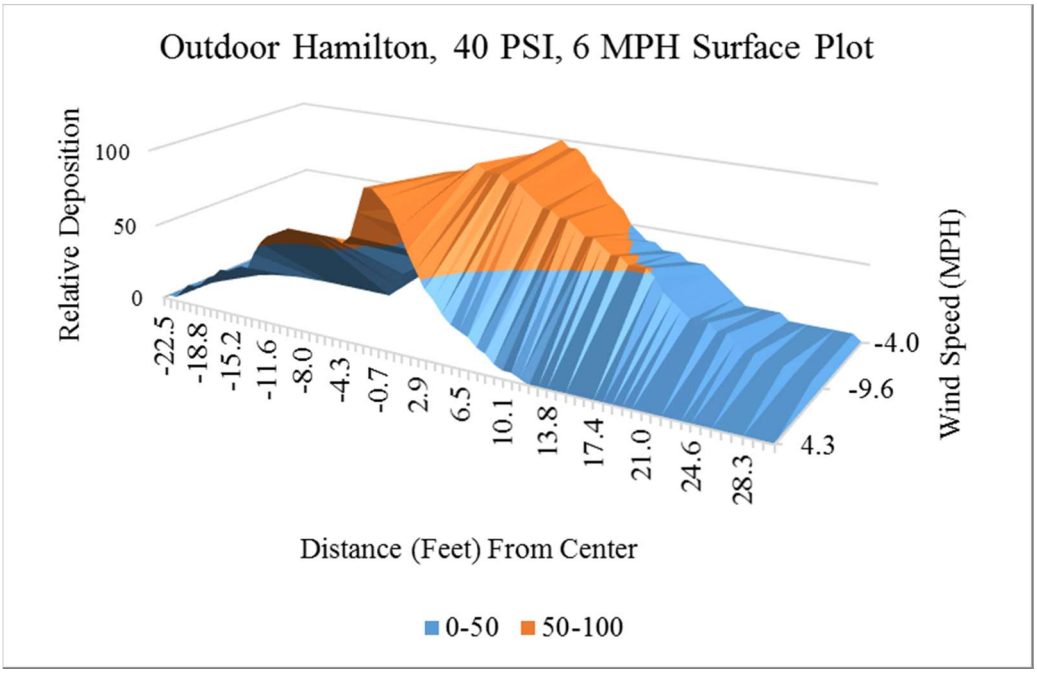

Figure 32. Surface plot of outdoor Hamilton.

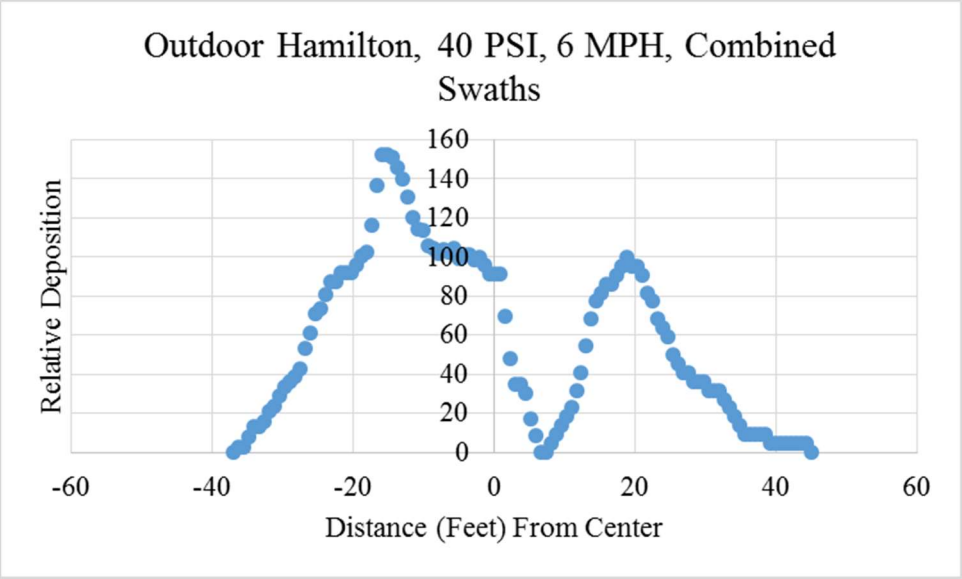

Figure 33. Simulated overlapped swath graph for outdoor Hamilton.

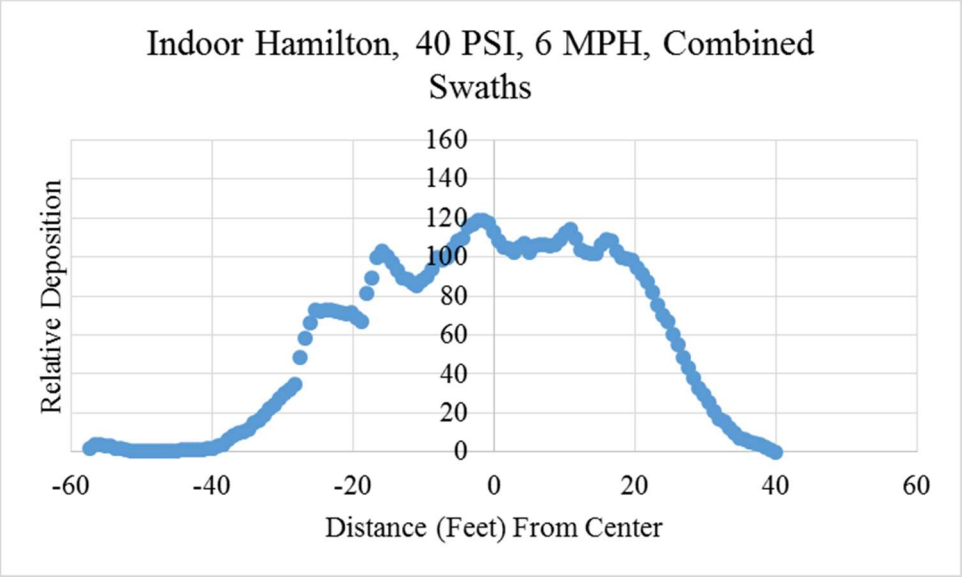

Figure 34. Simulated overlapped swath graph for indoor Hamilton.

CHAPTER V

CONCLUSION

Coefficient of Variation and Christiansen's Uniformity

The methods explained in this paper yielded an effective way to visualize spray distribution patterns that was also useful for statistically analyzing the effects of testing location, varying nozzle model, speed, and pressure on spray patterns. From the CU and CV data, it can be concluded that varying the nozzle will change the smoothness of the relative spray deposition pattern. In addition, the nozzle environment will also have an impact. When looking at spray pattern curves, it appears that wind conditions play an integral part in spray patterns. Driving is another key factor that was not considered in this experiment that would impact the CVs and CUs. The 50% lines were aligned as close as possible when the overlaps were simulated. This perfect alignment does not often occur during actual driving. It is very unlikely that a sprayer operator will know where the deposition of his or her spray pattern is at 50%. It is also unlikely that even if the operator knew where the 50% point occurred, that the operator is able to drive the spraying vehicle where the 50% points overlap perfectly without the help of an automated guidance and/or steering system. Using a computer system, more simulated overlaps could be

formed from just the three replications by randomizing the three replications or just varying the three replications and using different combinations of layouts. This method would be useful to further investigate how a CU may vary in a field on a given day of spraying.

Overall Width

The only nozzles that met or exceeded manufacturer's specifications for width both indoors and outdoors were the KLC 18 and KLC 36 nozzles. The Hamilton nozzle least squares means estimates were consistently below manufacturer estimates. These discrepancies show that work needs to be done among the manufacturers to ensure accurate width estimates to benefit the consumers. Looking at the least squares means estimates as well as the relative deposition curves reveals that the 5880 consistently yielded the widest widths, up to 59 feet outdoors and 49 feet indoors. The increase in width from indoors to outdoors is most likely due to wind effects. However, the application rate is not changing, therefore streaking is probably likely due to inconsistent deposition rates across the width of the nozzle swath. It was surprising that not all nozzles were significantly affected by either setting, pressure, speed, or a combination of those factors. Spray width is theoretically a function of pressure, but only the XP 25 had a significant interaction of setting and pressure. In addition, only the XT 024 had a significant effect of setting and the 5880 had a significant interaction of setting and speed. Perhaps the lack of significant effects and interactions was due to an insufficient range of pressures tested and winds encountered. Finally, just because the difference in width is not statistically significant in these tests does not mean it is not important for users to be aware of it. The difference of only one foot may lead to the presence or the lack of streaking or unsprayed land.

Effective Width

Effective width least squares estimates were lower than manufacturers' width estimates for every nozzle tested. Manufacturers are most likely just measuring the full width of the spray in ideal operating conditions. Nozzle operators need to know the difference between effective width and advertised with, and change operating practices accordingly. In addition, changing the location, pressure, or speed, or a combination, was a significant factor in changing the effective width of many of the nozzles. These factors are important to consider while spraying to effectively cover the intended spraying area.

Area

While the results for the area proved interesting due to the variety of statistically significant effects and interactions, the results must be taken with caution because the area is also affected by droplet size and fluorescent response of the water mixture used for testing. The same nozzle and pressure tests could be conducted in different wind conditions, and a more accurate picture of the effect of wind on application rates could be formed.

Width Offset

Statistical analysis showed that only two lower pressure nozzles (5880 and KLC 18) were affected by moving the testing from outdoors to indoors. Therefore, how much the midpoint of the width moves from wind conditions is not an important factor to consider for most boomless nozzles operated at a pressure of 40 psi or higher.

Ratio Skew

High pressure nozzles exhibited significant nozzle by setting and pressure by speed interactions, while the low pressure nozzles exhibited a significant nozzle by setting interaction. Therefore, the combination of testing location and nozzle model will make an impact on the skew of relative deposition patterns for most nozzles. In addition, the combination of pressure and speed was found to be significant for the high pressure nozzles. This may have been due to imperfections in either nozzle manufacturing or setup of the nozzle. Future testing will require

more extensive pre-testing of nozzles to ensure proper setup in an attempt to reduce the pressure and speed interaction. Testing of multiple nozzles of the same model may identify quality issues leading to ratio skew.

Overall Experiment

Overall, the testing method for this experiment proved effective. Statistically significant results were evident for many of the observed variables. However, testing was quite labor intensive, with approximately three weeks of work required to conduct all sprayer trials, and two more weeks of running string through the fluorometer were required. A simulated wind environment spray stand or spray table designed for boomless nozzles may ease the time and labor requirements. In addition, the fluorometer was prone to tangling the string. Over seven miles of string was run through the fluorometer. The entanglement of substantial amounts of string resulted in time lost as the string had to be reeled in again and the fluorometer restarted. A new testing medium that would be less prone to malfunctions would significantly increase the ease and efficiency of testing. For practical purposes, many of the methods here cannot be used by a general nozzle user. New methods that are easy to conduct need to be considered. Overall, the objectives and questions outlined at the beginning of this thesis were met:

- A method was developed for analyzing model performance.
- Christiansen's Uniformity Coefficient and coefficient of variation were used to evaluate pattern uniformity.
- How does the overall width and effective width of each nozzle in this study compare to manufacturer's specifications? Overall width was inconsistent but usually close to manufacturer specifications, while effective width was always lower.

- Does changing nozzle design, pressure, and vehicle speed effect performance? Yes, significant effects were observed in many of the variables analyzed in this study.

Future Research

Future areas of boomless nozzle research include investigating the application rates and a more drift-specific study. Correlation of fluorescence within application rate is dependent on droplet size distribution (Whitney and Roth). Therefore, the method described in this paper is not an accurate tool for specifically investigating application rate. If droplet sizes were measured and deemed to be approximately equal, looking at relative deposition curve areas would be sufficient for investing application rates. In addition, a medium for measuring drift from boomless nozzles would be very important, especially for sensitive mixtures that could kill or harm crops that the spray drifts onto. Moreover, the string method for analyzing patterns proved cumbersome. A new, easier, more reliable method would be useful and significantly increase the speed at which research can be conducted.

REFERENCES

Agri-Jet Flat Spray Nozzles. W.L Hamilton & Company. "Operating Data for 180 Degree Nozzles." Provided in nozzle packaging.

ASAE S327.4. July 2012 (R2016). Terminology and Definitions for Applications of Crop or Forestry Production and Protective Agents. American Society of Agricultural and Biological Engineers. P. 6. 4.13.

ASAE S341.4. Dec 2009 (R2015). Procedure for Measuring Distribution Uniformity and Calibrating Granular Broadcast Spreaders. American Society of Agricultural and Biological Engineers. P. 6.

Dickey, D. A. 2007. PROC MIXED: Underlying Ideas with Examples. NC State University, Raleigh, NC. Accessed Online. http://analytics.ncsu.edu/sesug/2007/SA07.pdf, 13.

Dibble, J. E., R. G. Curley, and N. B. Akesson. 1958. Boom and Broadcast Sprayers: Comparative field and laboratory study of spray distribution as applied by two types of sprayers on spotted alfalfa aphid. *California Agriculture*, January, 1958: 6-10.

Kees, G. 2008. Field Evaluation of a Constant-Rate Herbicide Sprayer for ATVs and UTVs. Tech. Rep. 0824-2802-MTDC. Missoula, MT: USDA Forest Service, Missoula Technology and Development Center. P. 18.

Krishnan, P., I. Gal, L. J. Kemble, and S. L. Gottfried. 1993. Effect of Sprayer Bound and Wind Condition on Spray Pattern Displacement of TJ60-8004 Fan Nozzles. Trans. ASAE 36(4): 997-1000.

Miller, J. H. 1990. Spray Distribution of Boomless Nozzles: The Boomjet 5880, Radiarc and Boom Buster. USDA Forest Service, Southern Forest Experiment Station. Auburn, AL.

Nuyttens, D., M. D. Schampheleire, W. Steurbaut, K. Baetens, P. Verboven, B. NicolaÏ, H. Ramon, and B. Sonck. 2006. Experimental Study of Factors Influencing the Risk of Drift from Field Sprayers, Part 1: Meteorological Conditions. *Aspects of Applied Biology*, 77.

Nuyttens, D., M. D. Schampheleire, W. Steurbaut, K. Baetens, P. Verboven, B. NicolaÏ, H. Ramon, and B. Sonck. 2006. Experimental Study of Factors Influencing the Risk of Drift from Field Sprayers, Part 2: Spray Application Technique. *Aspects of Applied Biology*, 77.

Pasta, D. J. M. D. 2011. Those Confounded Interactions: Building and Interpreting a Model with Many Potential Confounders and Interactions. Paper 347-2011. ICON Late Phase & Outcomes Research, San Francisco, CA. 7.

Pentair Hypro Boom X Tender Series. Form L-1484 (10/12). Provided in nozzle packaging.

Regan, R. 1987. Irrigation Practices: Measuring Sprinkler System Application Uniformity. Ornamentals Northwest Archives. 11(1): 10-12.

Spraying Systems Co. Data sheet 5880. Rev. No. 1. "BoomJet Boomless Flat Spray Nozzle. Provided in nozzle packaging.

Spraying Systems Co. Data sheet 6797. Rev. No. 1. Type KLC FieldJet Nozzle Gallons per acre. Accessed at http://www.sprayerdepot.com/core/media/media.nl/id.112098/c.3609571/.f?h=e78ce38847b83f7efb02&resizeid=-9&resizeh=800&resizew=800.

Smith, D. B. and D. D. Plummer. 1984. Broadcast Spray Deposit Evaluations at Sprayer Speeds up to 12 km/h. Trans. ASAE 27(3): 674-679.

Whitney, R. W. and L. O. Roth. 1985. String Collectors for Spray Pattern Analysis. Trans. ASAE 28(6): 1749-1753.

Wolf, R. and D. Peterson. 2009. An Evaluation of ATV-Mounted Boomless Spray Nozzles for Weed Control. Kansas State University Agricultural Experiment Station and Cooperative Extension Service. EP156.

"XP BoomJet Boomless Flat Spray Nozzles." Table Data Sheet. Accessed at http://teejet.it/media/bc303f7b-2038-48df-805e-bb6a56b90193-CAT50-US_LoRes_p033.pdf.

APPENDIX A.

CODE INPUTTED TO SAS® SOFTWARE COPYRIGHT © 2012 FOR ANALYSIS

OF

EFFECTIVE WIDTH

```
proc mixed covtest nobound;
title 'Effective Width Evaluation by Nozzle';
by nozzle;
class setting pressure speed  replication;

model effective=setting
pressure    setting*pressure
speed setting*speed
pressure*speed    setting*pressure*speed/residual ddfm=kr;

lsmeans setting
pressure    setting*pressure
speed setting*speed
pressure*speed    setting*pressure*speed;
*Effective is the transformed effective width variable;
*Pressure is the nozzle pressure, speed is the tractor speed,
setting is the test location, nozzle is the nozzle model,
replication is the test replication;
*you will need to input variables to complete this code;
*you will need to input a file or data to complete this code;

random setting*replication;
run;
```

APPENDIX B.

CODE INPUTTED TO SAS® SOFTWARE COPYRIGHT © 2012 FOR ANALYSIS

OF

WIDTH

```
proc sort;
by type;
run;
proc sort;
by nozzle;
run;
ods graphics on;
proc mixed covtest nobound;
title 'Johnson Width Evaluation by Nozzle';
by nozzle;
class setting pressure speed replication;

model johnsonwidth=setting    pressure    setting*pressure
speed setting*speed     pressure*speed
setting*pressure*speed/residual ddfm=kr;

lsmeans setting   pressure    setting*pressure  speed
setting*speed     pressure*speed    setting*pressure*speed/CL;
*Johnsonwidth is the transformed width of each swath variable;
*Pressure is the nozzle pressure, speed is the tractor speed,
setting is the test location, nozzle is the nozzle model,
replication is the test replication;
*you will need to input variables to complete this code;
*you will need to input a file or data to complete this code;

random setting*replication;
run;
```

APPENDIX C.

CODE INPUTTED TO SAS® SOFTWARE COPYRIGHT © 2012 FOR ANALYSIS

OF

AREA

```
proc sort;
by nozzle;
run;
ods graphics on;
proc mixed covtest nobound;
title 'Area Evaluation by Nozzle';
by nozzle;
class setting pressure speed replication;

model johnson=setting   pressure
      setting*pressure
speed setting*speed
pressure*speed    setting*pressure*speed
/residual ddfm=kr;

lsmeans setting   pressure
      setting*pressure
speed setting*speed
pressure*speed    setting*pressure*speed;
*Johnson is the transformed area variable;
*Pressure is the nozzle pressure, speed is the tractor speed,
setting is the test location, nozzle is the nozzle model,
replication is the test replication;
*you will need to input variables to complete this code;
*you will need to input a file or data to complete this code;

random setting*replication;
run;
```

APPENDIX D.

CODE INPUTTED TO SAS® SOFTWARE COPYRIGHT © 2012 FOR ANALYSIS

OF

WIDTH OFFSET

BY TYPE:

```
proc sort;
by type;
run;
ods graphics on;
proc mixed covtest nobound;
title 'Widthoffset Evaluation by Type';
by type;
class setting pressure speed nozzle replication;

model johnson=nozzle    setting     nozzle*setting    pressure
nozzle*pressure   setting*pressure  nozzle*setting*pressure speed
nozzle*speed      setting*speed     nozzle*setting*speed
pressure*speed    nozzle*pressure*speed   setting*pressure*speed
nozzle*setting*pressure*speed/residual ddfm=kr;

lsmeans nozzle    setting     nozzle*setting    pressure
nozzle*pressure   setting*pressure  nozzle*setting*pressure
speed nozzle*speed      setting*speed     nozzle*setting*speed
pressure*speed    nozzle*pressure*speed   setting*pressure*speed
nozzle*setting*pressure*speed;
*Johnson is the transformed width offset variable;
*Pressure is the nozzle pressure, speed is the tractor speed,
setting is the test location, nozzle is the nozzle model,
replication is the test replication;
*you will need to input variables to complete this code;
*you will need to input a file or data to complete this code;

random setting*replication;
run;
```

BY NOZZLE:

```
proc sort;
by type;
run;
proc sort;
by nozzle;
run;
ods graphics on;
proc mixed covtest nobound;
title 'Johnson Widthoffset Evaluation by Nozzle';
by nozzle;
class setting pressure speed replication;

model johnson=setting   pressure    setting*pressure
speed setting*speed     pressure*speed
setting*pressure*speed/residual ddfm=kr;

lsmeans setting   pressure    setting*pressure  speed
setting*speed     pressure*speed    setting*pressure*speed;
*Johnsonwidth is the transformed width of each swath variable;
*Pressure is the nozzle pressure, speed is the tractor speed,
setting is the test location, nozzle is the nozzle model,
replication is the test replication;
*you will need to input variables to complete this code;
*you will need to input a file or data to complete this code;

random setting*replication;
run;
```

APPENDIX E.

CODE INPUTTED TO SAS® SOFTWARE COPYRIGHT © 2012 FOR ANALYSIS

OF

RATIO SKEW

BY TYPE:

```
proc sort;
by type;
run;
ods graphics on;
proc mixed covtest nobound;
title 'Ratio Skew Evaluation by Type';
by type;
class setting pressure speed nozzle replication;

model johnson1=nozzle   setting     nozzle*setting    pressure
nozzle*pressure   setting*pressure  nozzle*setting*pressure
speed nozzle*speed      setting*speed     nozzle*setting*speed
pressure*speed    nozzle*pressure*speed   setting*pressure*speed
nozzle*setting*pressure*speed
/residual ddfm=kr;

lsmeans nozzle    setting     nozzle*setting    pressure
nozzle*pressure   setting*pressure  nozzle*setting*pressure
speed nozzle*speed      setting*speed     nozzle*setting*speed
pressure*speed    nozzle*pressure*speed   setting*pressure*speed
nozzle*setting*pressure*speed;
*Johnson is the transformed width offset variable;
*Pressure is the nozzle pressure, speed is the tractor speed,
setting is the test location, nozzle is the nozzle model,
replication is the test replication;
*you will need to input variables to complete this code;
*you will need to input a file or data to complete this code;

random setting*replication;
run;
```

BY NOZZLE:

```
proc sort;
by type;
run;
proc sort;
by nozzle;
run;
ods graphics on;
proc mixed covtest nobound;
title 'Johnson Ratio Skew Evaluation by Nozzle';
by nozzle;
class setting pressure speed replication;

model johnson2=setting  pressure    setting*pressure
speed setting*speed     pressure*speed    setting*pressure*speed
/residual ddfm=kr;

lsmeans setting   pressure    setting*pressure  speed
setting*speed     pressure*speed setting*pressure*speed;
*Johnson2 is the transformed ratio skew as calculated from each run;
*Pressure is the nozzle pressure, speed is the tractor speed,
setting is the test location, nozzle is the nozzle model,
replication is the test replication;
*you will need to input variables to complete this code;
*you will need to input a file or data to complete this code;

random setting*replication;
run;
```

APPENDIX F.

UNBOUNDED JOHNSON DISTRIBUTION FORMULATED USING JMP®

SOFTWARE COPYRIGHT © 2016 FOR ANALYSIS OF

EFFECTIVE WIDTH

$$
\text{If}\left(\begin{array}{lll}
Nozzle == \text{"XT024"} & \Rightarrow & \text{ArcSinH}\left(\dfrac{\left(Effective\ Width - 30.972682344\right)}{0.0001112786}\right) \cdot 3.2336168789 + 39.713530741 \\
Nozzle == \text{"XP40"} & \Rightarrow & \text{ArcSinH}\left(\dfrac{\left(Effective\ Width - 24.43777682\right)}{0.000045736}\right) \cdot 2.0014652866 + 24.286399137 \\
Nozzle == \text{"XP25"} & \Rightarrow & \text{ArcSinH}\left(\dfrac{\left(Effective\ Width - 4.4951728567\right)}{4.4861455e\text{-}6}\right) \cdot 5.816575807 + -90.58596314 \\
Nozzle == \text{"KLC36"} & \Rightarrow & \text{ArcSinH}\left(\dfrac{\left(Effective\ Width - 23.510062095\right)}{0.000053576}\right) \cdot 2.462280712 + 30.384021116 \\
Nozzle == \text{"KLC18"} & \Rightarrow & \text{ArcSinH}\left(\dfrac{\left(Effective\ Width - 1.9616317588\right)}{0.0000151282}\right) \cdot 4.9124464449 + -69.86423468 \\
Nozzle == \text{"Ham"} & \Rightarrow & \text{ArcSinH}\left(\dfrac{\left(Effective\ Width - 33.279622987\right)}{0.0001634789}\right) \cdot 5.1675398687 + 63.259862795 \\
\text{else} & \Rightarrow & .
\end{array}\right)
$$

APPENDIX G.

UNBOUNDED JOHNSON DISTRIBUTION FORMULATED USING JMP®

SOFTWARE COPYRIGHT © 2016 FOR ANALYSIS OF

WIDTH

$$
\text{If}\left(\begin{array}{lll}
Nozzle == \text{"XP40"} & \Rightarrow & \text{ArcSinH}\left(\frac{\left(Width - 25.943180865\right)}{3.3775039859}\right) \cdot 1.1529064352 + -1.487298352 \\
Nozzle == \text{"XT024"} & \Rightarrow & \text{ArcSinH}\left(\frac{\left(Width - 22.354158548\right)}{1.0156391e\text{-}6}\right) \cdot 1.4207198956 + -23.70055956 \\
Nozzle == \text{"XP25"} & \Rightarrow & \text{ArcSinH}\left(\frac{\left(Width - 23.235978789\right)}{2.0711109175}\right) \cdot 1.0027287654 + -1.655824927 \\
Nozzle == \text{"KLC36"} & \Rightarrow & \text{ArcSinH}\left(\frac{\left(Width - 29.302404377\right)}{3.6726495041}\right) \cdot 0.8260542297 + -0.515220177 \\
Nozzle == \text{"KLC18"} & \Rightarrow & \text{ArcSinH}\left(\frac{\left(Width - 18.45603509\right)}{4.7503423637}\right) \cdot 1.4107208983 + -2.340761736 \\
Nozzle == \text{"Ham"} & \Rightarrow & \text{ArcSinH}\left(\frac{\left(Width - 19.737515638\right)}{1.0894744e\text{-}7}\right) \cdot 1.6894885814 + -33.14234743 \\
Nozzle == \text{"5880"} & \Rightarrow & \text{ArcSinH}\left(\frac{\left(Width - 29.037420071\right)}{3.7792456e\text{-}6}\right) \cdot 2.2231251907 + -36.0798427 \\
\text{else} & \Rightarrow & .
\end{array}\right)
$$

APPENDIX H.

UNBOUNDED JOHNSON DISTRIBUTION FORMULATED USING JMP®

SOFTWARE COPYRIGHT © 2016 FOR ANALYSIS OF

AREA

$$
\text{If}\left(\begin{array}{lll}
Nozzle == \text{"KLC18"} & \Rightarrow & \text{ArcSinH}\left(\frac{\left(areas - 618.09233203\right)}{0.0010700156}\right) \cdot 2.4689382571 + -35.30694797 \\
Nozzle == \text{"XP25"} & \Rightarrow & \text{ArcSinH}\left(\frac{\left(areas - 642.68418185\right)}{0.0001856835}\right) \cdot 3.1553255886 + -50.81393168 \\
Nozzle == \text{"XP40"} & \Rightarrow & \text{ArcSinH}\left(\frac{\left(areas - 690.19940908\right)}{0.0001239543}\right) \cdot 3.2580816276 + -54.10195683 \\
Nozzle == \text{"XT024"} & \Rightarrow & \text{ArcSinH}\left(\frac{\left(areas - 1388.2655758\right)}{567.35175381}\right) \cdot 2.1288050863 + -0.798236042 \\
\text{else} & \Rightarrow & .
\end{array}\right)
$$

APPENDIX I.

UNBOUNDED JOHNSON DISTRIBUTION FORMULATED USING JMP®

SOFTWARE COPYRIGHT © 2016 FOR ANALYSIS OF

WIDTH MIDPOINT DISTANCE FROM CENTER (WIDTH OFFSET)

BY TYPE:

$$\text{If}\left(\begin{array}{lll} \textit{Type} == \text{"high"} & \Rightarrow & \text{ArcSinH}\left(\frac{\left(\textit{widthoffset} - 1.1388557605\right)}{1.36243832}\right) \cdot 0.7472700326 + -0.050920851 \\ \textit{Type} == \text{"low"} & \Rightarrow & \text{ArcSinH}\left(\frac{\left(\textit{widthoffset} - 1.1445153494\right)}{1.3420835868}\right) \cdot 0.7183800479 + 0.2376511208 \\ \text{else} & \Rightarrow & . \end{array}\right)$$

BY NOZZLE:

$$
\text{If}\left(\begin{array}{lll}
Nozzle == \text{"XT024"} & \Rightarrow & \text{ArcSinH}\left(\frac{\left(widthoffset - 0.5078875652\right)}{1.9007532222}\right) \cdot 1.0230145633 + -0.411228192 \\
Nozzle == \text{"XP40"} & \Rightarrow & \text{ArcSinH}\left(\frac{\left(widthoffset - 0.4817790384\right)}{0.862160423}\right) \cdot 0.7008387368 + -0.392201932 \\
Nozzle == \text{"XP25"} & \Rightarrow & \text{ArcSinH}\left(\frac{\left(widthoffset - 1.7449878475\right)}{0.9757146615}\right) \cdot 0.728017536 + 0.1071621485 \\
Nozzle == \text{"KLC36"} & \Rightarrow & \text{ArcSinH}\left(\frac{\left(widthoffset - 0.8534937563\right)}{0.6824973697}\right) \cdot 0.5860815166 + -0.03780425 \\
Nozzle == \text{"KLC18"} & \Rightarrow & \text{ArcSinH}\left(\frac{\left(widthoffset - 2.0341414218\right)}{1.5130838118}\right) \cdot 0.9612987659 + 0.8486803734 \\
Nozzle == \text{"Ham"} & \Rightarrow & \text{ArcSinH}\left(\frac{\left(widthoffset - 0.8269891803\right)}{2.544877632}\right) \cdot 0.814758471 + 0.0473681873 \\
Nozzle == \text{"5880"} & \Rightarrow & \text{ArcSinH}\left(\frac{\left(widthoffset - 0.8538199961\right)}{2.7921502063}\right) \cdot 0.8917570277 + 0.1514192812 \\
\text{else} & \Rightarrow & .
\end{array}\right)
$$

APPENDIX J.

UNBOUNDED JOHNSON DISTRIBUTION FORMULATED USING JMP®

SOFTWARE COPYRIGHT © 2016 FOR ANALYSIS OF RATIO SKEW

BY TYPE:

$$\text{If}\left(\begin{array}{lll} \textit{Type} == \text{"low"} & \Rightarrow & \text{ArcSinH}\left(\dfrac{\left(\textit{Left to right ratio} - 0.8366301782\right)}{0.1267833427}\right) \bullet 0.6582934369 + -0.277264286 \\ \textit{Type} == \text{"high"} & \Rightarrow & \text{ArcSinH}\left(\dfrac{\left(\textit{Left to right ratio} - 0.8447892177\right)}{0.2497903464}\right) \bullet 0.954453971 + -0.230176671 \\ \text{else} & \Rightarrow & . \end{array}\right)$$

BY NOZZLE:

$$
\text{If}\left(\begin{array}{lll}
\textit{Nozzle} == \text{"XT024"} & \Rightarrow & \text{ArcSinH}\left(\dfrac{\left(\textit{Left to right ratio} - 0.6071013312\right)}{0.6186950021}\right) \cdot 2.3860464227 + -0.861857102 \\
\textit{Nozzle} == \text{"XP40"} & \Rightarrow & \text{ArcSinH}\left(\dfrac{\left(\textit{Left to right ratio} - 1.0072379406\right)}{0.2762123201}\right) \cdot 1.2624524471 + 0.4896138269 \\
\textit{Nozzle} == \text{"XP25"} & \Rightarrow & \text{ArcSinH}\left(\dfrac{\left(\textit{Left to right ratio} - 0.7323693536\right)}{0.1881253707}\right) \cdot 0.8211481132 + -0.603951155 \\
\textit{Nozzle} == \text{"KLC36"} & \Rightarrow & \text{ArcSinH}\left(\dfrac{\left(\textit{Left to right ratio} - 0.8605461516\right)}{0.1001172702}\right) \cdot 0.6077108567 + -0.020304027 \\
\textit{Nozzle} == \text{"KLC18"} & \Rightarrow & \text{ArcSinH}\left(\dfrac{\left(\textit{Left to right ratio} - 0.7321841563\right)}{0.0954891169}\right) \cdot 0.5883869836 + -0.696540584 \\
\textit{Nozzle} == \text{"Ham"} & \Rightarrow & \text{ArcSinH}\left(\dfrac{\left(\textit{Left to right ratio} - 0.9194375217\right)}{0.1671016414}\right) \cdot 0.6916955557 + -0.287907825 \\
\textit{Nozzle} == \text{"5880"} & \Rightarrow & \text{ArcSinH}\left(\dfrac{\left(\textit{Left to right ratio} - 0.9343858653\right)}{0.2118466931}\right) \cdot 0.9991452681 + -0.026696667 \\
\text{else} & \Rightarrow & .
\end{array}\right)
$$

APPENDIX K.

EFFECTIVE WIDTH LEAST SQUARES MEANS RESULTS IN FEET

Press. (PSI)	Speed (MPH)	5880		KLC 18		KLC 36		Ham		XP 25		XP 40		XT 024	
		In.	Out.	In.	Out.	In.	Out.	In.	Out.	In.	Out.	In.	Out.	In.	Out.
20	4	20	21	13	14	18	17	OUTSIDE TESTED RANGE							
	6	15	23	14	13	18	17								
	8	17	15	12	11	15	11								
30	4	24	19	14	17	19	18								
	6	21	16	14	16	19	16								
	8	20	15	13	10	17	14								
40	4	25	21	15	14	21	18								
	6	22	19	14	11	18	18	19	16	18	18	22	19	22	18
	8	21	18	12	15	18	14	15	13	17	18	19	18	18	20
	10	OUTSIDE TESTED RANGE						12	18	17	17	20	16	18	17
50	6							19	13	19	19	22	21	19	20
	8							18	16	19	18	21	18	17	17
	10							17	13	19	14	21	20	16	15
60	6							20	15	19	16	OUTSIDE TESTED RANGE		24	21
	8							18	18	20	16			18	18
	10							18	12	17	17			21	18

APPENDIX L.

WIDTH LEAST SQUARES MEANS RESULTS IN FEET

Press. (PSI)	Speed (MPH)	5880 In.	5880 Out.	KLC 18 In.	KLC 18 Out.	KLC 36 In.	KLC 36 Out.	Ham In.	Ham Out.	XP 25 In.	XP 25 Out.	XP 40 In.	XP 40 Out.	XT 024 In.	XT 024 Out.
20	4	63	61	30	38	30	41	OUTSIDE TESTED RANGE							
	6	53	87	28	33	30	28								
	8	49	57	24	27	27	31								
30	4	68	64	26	33	32	35								
	6	62	81	37	37	35	28								
	8	46	81	23	33	31	32								
40	4	77	64	35	39	33	35								
	6	57	65	28	35	38	33	45	50	30	34	34	37	33	28
	8	51	53	28	29	31	32	31	48	27	30	32	30	29	31
	10	OUTSIDE TESTED RANGE						30	34	24	48	32	31	26	28
50	6							36	42	27	27	31	33	32	32
	8							34	37	29	29	32	32	29	39
	10							31	46	28	32	30	31	29	36
60	6							48	42	31	29	OUTSIDE TESTED RANGE		35	36
	8							40	34	30	26			29	33
	10							36	33	26	26			30	42

APPENDIX M.

AREA (RELATIVE) LEAST SQUARES MEANS RESULTS

Press. (PSI)	Speed (MPH	5880		KLC 18		KLC 36		Ham		XP 25		XP 40		XT 024	
		In.	Out.	In.	Out.	In.	Out.	In.	Out.	In.	Out.	In.	Out.	In.	Out.
20	4	1870	2138	1841	1324	1406	1637	OUTSIDE TESTED RANGE							
	6	1673	2177	1813	1238	1586	1468								
	8	1752	1636	1836	1140	1696	1272								
30	4	1803	2163	1812	1536	1720	1738								
	6	1185	1982	1600	1557	1919	1476								
	8	2104	1810	1667	1126	1749	1328								
40	4	1688	2131	1951	1423	1672	1676								
	6	1492	2135	1406	1179	1637	1719	1502	1603	1440	1582	1667	1669	1536	1571
	8	1814	1957	1648	1365	1699	1482	1497	1476	1946	1577	1771	1672	1598	1725
	10	OUTSIDE TESTED RANGE						1748	1719	1678	1602	1913	1315	1502	1586
50	6							2113	1509	1424	1613	1712	1810	1567	1632
	8							1627	1510	1633	1625	1894	1525	1805	1616
	10							1741	1392	2005	1392	1792	1681	2033	1486
60	6							1754	1549	1427	1583	OUTSIDE TESTED RANGE		1364	1934
	8							1994	1745	1445	1397			1285	1653
	10							1786	1321	1422	1508			1510	1665

APPENDIX N.

WIDTH OFFSET LEAST SQUARES MEANS RESULTS IN FEET

Press. (PSI)	Speed (MPH	5880		KLC 18		KLC 36		Ham		XP 25		XP 40		XT 024	
		In.	Out.	In.	Out.	In.	Out.	In.	Out.	In.	Out.	In.	Out.	In.	Out.
20	4	-1.0	-5.5	1.8	-1.4	1.4	0.8	OUTSIDE TESTED RANGE							
	6	1.8	-0.7	-0.4	-1.8	1.1	2.1								
	8	0.0	-1.3	1.0	-2.4	0.6	0.6								
30	4	1.6	4.8	1.0	-3.8	1.2	-0.6								
	6	4.4	-1.6	1.8	-1.4	0.6	-0.1								
	8	1.4	-2.2	1.1	-0.2	1.0	0.1								
40	4	0.1	-0.3	1.5	0.4	1.4	6.5								
	6	0.8	-3.2	1.2	0.7	1.0	1.2	-0.4	2.5	2.3	0.7	1.1	0.4	1.9	2.5
	8	1.9	3.6	3.0	1.0	0.6	-0.2	0.9	2.5	1.4	-0.7	0.6	0.4	0.9	3.2
	10	OUTSIDE TESTED RANGE						0.8	1.6	1.6	3.6	0.7	1.1	0.8	2.8
50	6							1.1	-0.8	1.9	0.3	0.6	0.9	0.5	0.7
	8							1.2	-3.6	1.7	0.1	0.6	1.8	1.2	0.0
	10							1.4	-1.3	1.2	1.1	1.0	0.5	1.2	1.7
60	6							1.9	0.6	1.7	2.7	OUTSIDE TESTED RANGE		1.6	0.7
	8							0.5	2.5	2.7	3.3			1.2	1.4
	10							2.1	-3.4	1.8	0.6			-0.5	2.9

APPENDIX O.

RATIO SKEW LEAST SQUARES MEANS RESULTS

Press. (PSI)	Speed (MPH)	5880		KLC 18		KLC 36		Ham		XP 25		XP 40		XT 024	
		In.	out.	In.	out.	In.	out.	In.	out.	In.	out.	In.	out.	In.	out.
20	4	1.0	1.2	0.7	1.3	0.9	1.0	OUTSIDE TESTED RANGE							
	6	0.9	0.9	0.9	1.0	0.9	0.5								
	8	1.1	1.2	0.9	1.2	0.9	0.7								
30	4	0.9	0.7	0.8	1.3	0.9	1.0								
	6	0.8	0.8	0.7	1.3	0.9	1.0								
	8	0.9	1.0	0.8	0.8	0.9	0.9								
40	4	1.0	0.9	0.8	0.8	0.8	0.4								
	6	1.0	1.1	0.8	0.8	0.9	0.8	1.0	0.8	0.8	1.1	1.0	0.8	0.9	0.6
	8	0.9	0.7	0.8	1.0	0.9	1.1	0.9	1.0	1.0	1.2	0.9	1.1	1.0	0.6
50	10	OUTSIDE TESTED RANGE						0.9	0.9	0.8	0.7	0.8	0.7	0.9	0.8
	6							1.0	1.1	0.8	1.1	1.0	0.9	0.9	0.8
	8							0.9	1.5	0.9	1.5	1.0	0.6	0.8	0.7
	10							0.9	1.5	0.9	1.0	1.0	0.9	1.0	0.7
60	6							1.0	1.0	0.9	0.7	OUTSIDE TESTED RANGE		0.9	0.8
	8							0.9	0.8	0.8	0.6			0.9	0.9
	10							0.9	1.6	0.8	1.3			1.0	0.9

APPENDIX P.

ARDUINO CODE USED FOR WEATHER STATION

CODE WAS MODIFIED FROM CODE FOUND AT WWW.SPARKFUN.COM

```
 */

#include <Wire.h> //I2C needed for sensors
#include "SparkFunMPL3115A2.h" //Pressure sensor - Search "SparkFun MPL3115" and install from Library Manager
#include "SparkFunHTU21D.h" //Humidity sensor - Search "SparkFun HTU21D" and install from Library Manager
#include <SoftwareSerial.h> //Needed for GPS
#include <TinyGPS++.h> //GPS parsing

TinyGPSPlus gps;

static const int RXPin = 5, TXPin = 4; //GPS is attached to pin 4(TX from GPS) and pin 5(RX into GPS)
SoftwareSerial ss(RXPin, TXPin);

MPL3115A2 myPressure; //Create an instance of the pressure sensor
HTU21D myHumidity; //Create an instance of the humidity sensor

//Hardware pin definitions
//-=-=-=-=-=-=-=-=-=-=-=-=-=-=-=-=-=-=-=-=-=-=-=-=-=-=-=-=-=-=-=-=-=-=-=-=-=-=-=-=
// digital I/O pins
const byte WSPEED = 3;
const byte RAIN = 2;
const byte STAT1 = 7;
const byte STAT2 = 8;
const byte GPS_PWRCTL = 6; //Pulling this pin low puts GPS to sleep but maintains RTC and RAM

// analog I/O pins
const byte REFERENCE_3V3 = A3;
const byte LIGHT = A1;
const byte BATT = A2;
const byte WDIR = A0;
//-=-=-=-=-=-=-=-=-=-=-=-=-=-=-=-=-=-=-=-=-=-=-=-=-=-=-=-=-=-=-=-=-=-=-=-=-=-=-=-=

//Global Variables
//-=-=-=-=-=-=-=-=-=-=-=-=-=-=-=-=-=-=-=-=-=-=-=-=-=-=-=-=-=-=-=-=-=-=-=-=-=-=-=-=
long lastSecond; //The millis counter to see when a second rolls by
byte seconds; //When it hits 60, increase the current minute
byte seconds_2m; //Keeps track of the "wind speed/dir avg" over last 2 minutes array of data
```

```
byte minutes; //Keeps track of where we are in various arrays of data
byte minutes_10m; //Keeps track of where we are in wind gust/dir over last 10 minutes array of data

long lastWindCheck = 0;
volatile long lastWindIRQ = 0;
volatile byte windClicks = 0;

//We need to keep track of the following variables:
//Wind speed/dir each update (no storage)
//Wind gust/dir over the day (no storage)
//Wind speed/dir, avg over 2 minutes (store 1 per second)
//Wind gust/dir over last 10 minutes (store 1 per minute)
//Rain over the past hour (store 1 per minute)
//Total rain over date (store one per day)

byte windspdavg[120]; //120 bytes to keep track of 2 minute average

#define WIND_DIR_AVG_SIZE 120
int winddiravg[WIND_DIR_AVG_SIZE]; //120 ints to keep track of 2 minute average
float windgust_10m[10]; //10 floats to keep track of 10 minute max
int windgustdirection_10m[10]; //10 ints to keep track of 10 minute max
volatile float rainHour[60]; //60 floating numbers to keep track of 60 minutes of rain

//These are all the weather values that wunderground expects:
int winddir = 0; // [0-360 instantaneous wind direction]
float windspeedmph = 0; // [mph instantaneous wind speed]
float windgustmph = 0; // [mph current wind gust, using software specific time period]
int windgustdir = 0; // [0-360 using software specific time period]
float windspdmph_avg2m = 0; // [mph 2 minute average wind speed mph]
int winddir_avg2m = 0; // [0-360 2 minute average wind direction]
float windgustmph_10m = 0; // [mph past 10 minutes wind gust mph ]
int windgustdir_10m = 0; // [0-360 past 10 minutes wind gust direction]
float humidity = 0; // [%]
float tempf = 0; // [temperature F]
float rainin = 0; // [rain inches over the past hour)] -- the accumulated rainfall in the past 60 min
volatile float dailyrainin = 0; // [rain inches so far today in local time]
//float baromin = 30.03;// [barom in] - It's hard to calculate baromin locally, do this in the agent
float pressure = 0;
//float dewptf; // [dewpoint F] - It's hard to calculate dewpoint locally, do this in the agent

float batt_lvl = 11.8; //[analog value from 0 to 1023]
float light_lvl = 455; //[analog value from 0 to 1023]

// volatiles are subject to modification by IRQs
volatile unsigned long raintime, rainlast, raininterval, rain;

//-=-=-=-=-=-=-=-=-=-=-=-=-=-=-=-=-=-=-=-=-=-=-=-=-=-=-=-=-=-=-=-=-=-=-=-=

//Interrupt routines (these are called by the hardware interrupts, not by the main code)
//-=-=-=-=-=-=-=-=-=-=-=-=-=-=-=-=-=-=-=-=-=-=-=-=-=-=-=-=-=-=-=-=-=-=-=-=
void rainIRQ()
// Count rain gauge bucket tips as they occur
// Activated by the magnet and reed switch in the rain gauge, attached to input D2
{
  raintime = millis(); // grab current time
  raininterval = raintime - rainlast; // calculate interval between this and last event

  if (raininterval > 10) // ignore switch-bounce glitches less than 10mS after initial edge
  {
```

```
    dailyrainin += 0.011; //Each dump is 0.011" of water
    rainHour[minutes] += 0.011; //Increase this minute's amount of rain

    rainlast = raintime; // set up for next event
  }
}

void wspeedIRQ()
// Activated by the magnet in the anemometer (2 ticks per rotation), attached to input D3
{
  if (millis() - lastWindIRQ > 10) // Ignore switch-bounce glitches less than 10ms (142MPH max
reading) after the reed switch closes
  {
    lastWindIRQ = millis(); //Grab the current time
    windClicks++; //There is 1.492MPH for each click per second.
  }
}


void setup()
{
  Serial.begin(9600);
  Serial.println("Weather Shield Example");

  ss.begin(9600); //Begin listening to GPS over software serial at 9600. This should be the default baud
of the module. added

  pinMode(STAT1, OUTPUT); //Status LED Blue
  pinMode(STAT2, OUTPUT); //Status LED Green

   pinMode(GPS_PWRCTL, OUTPUT); //added
  digitalWrite(GPS_PWRCTL, HIGH); //Pulling this pin low puts GPS to sleep but maintains RTC and
RAM added

  pinMode(WSPEED, INPUT_PULLUP); // input from wind meters windspeed sensor
  pinMode(RAIN, INPUT_PULLUP); // input from wind meters rain gauge sensor

  pinMode(REFERENCE_3V3, INPUT);
  pinMode(LIGHT, INPUT);

  //Configure the pressure sensor
  myPressure.begin(); // Get sensor online
  myPressure.setModeBarometer(); // Measure pressure in Pascals from 20 to 110 kPa
  myPressure.setOversampleRate(7); // Set Oversample to the recommended 128
  myPressure.enableEventFlags(); // Enable all three pressure and temp event flags

  //Configure the humidity sensor
  myHumidity.begin();

  seconds = 0;
  lastSecond = millis();

  // attach external interrupt pins to IRQ functions
  attachInterrupt(0, rainIRQ, FALLING);
  attachInterrupt(1, wspeedIRQ, FALLING);

  // turn on interrupts
  interrupts();
```

```
  Serial.println("Weather Shield online!");

}

void loop()
{
  //Keep track of which minute it is
  if(millis() - lastSecond >= 1000)
  {
    digitalWrite(STAT1, HIGH); //Blink stat LED

    lastSecond += 1000;

    //Take a speed and direction reading every second for 2 minute average
    if(++seconds_2m > 119) seconds_2m = 0;

    //Calc the wind speed and direction every second for 120 second to get 2 minute average
    float currentSpeed = get_wind_speed();
    windspeedmph = currentSpeed; //update global variable for windspeed when using the
printWeather() function
    //float currentSpeed = random(5); //For testing
    int currentDirection = get_wind_direction();
    windspdavg[seconds_2m] = (int)currentSpeed;
    winddiravg[seconds_2m] = currentDirection;
    //if(seconds_2m % 10 == 0) displayArrays(); //For testing

    //Check to see if this is a gust for the minute
    if(currentSpeed > windgust_10m[minutes_10m])
    {
      windgust_10m[minutes_10m] = currentSpeed;
      windgustdirection_10m[minutes_10m] = currentDirection;
    }

    //Check to see if this is a gust for the day
    if(currentSpeed > windgustmph)
    {
      windgustmph = currentSpeed;
      windgustdir = currentDirection;
    }

    if(++seconds > 59)
    {
      seconds = 0;

      if(++minutes > 59) minutes = 0;
      if(++minutes_10m > 9) minutes_10m = 0;

      rainHour[minutes] = 0; //Zero out this minute's rainfall amount
      windgust_10m[minutes_10m] = 0; //Zero out this minute's gust
    }

    //Report all readings every second
    printWeather();

    digitalWrite(STAT1, LOW); //Turn off stat LED
  }

  //delay(100);  changed this
  smartdelay(800); //wait 1 second, and gather gps data
```

```
}

//Calculates each of the variables that wunderground is expecting
//void calcWeather()
//while we delay for a given amount of time, gather gps data
static void smartdelay(unsigned long ms)
{
  unsigned long start = millis();
  do
  {
    while (ss.available())
    gps.encode(ss.read());
  } while (millis() - start < ms);
  }
  void calcWeather()
  {
  //Calc winddir
  winddir = get_wind_direction();

  //Calc windspeed
  //windspeedmph = get_wind_speed(); //This is calculated in the main loop on line 179

  //Calc windgustmph
  //Calc windgustdir
  //These are calculated in the main loop

  //Calc windspdmph_avg2m
  float temp = 0;
  for(int i = 0 ; i < 120 ; i++)
    temp += windspdavg[i];
  temp /= 120.0;
  windspdmph_avg2m = temp;

  //Calc winddir_avg2m, Wind Direction
  //You can't just take the average. Google "mean of circular quantities" for more info
  //We will use the Mitsuta method because it doesn't require trig functions
  //And because it sounds cool.
  //Based on: http://abelian.org/vlf/bearings.html
  //Based on: http://stackoverflow.com/questions/1813483/averaging-angles-again
  long sum = winddiravg[0];
  int D = winddiravg[0];
  for(int i = 1 ; i < WIND_DIR_AVG_SIZE ; i++)
  {
    int delta = winddiravg[i] - D;

    if(delta < -180)
      D += delta + 360;
    else if(delta > 180)
      D += delta - 360;
    else
      D += delta;

    sum += D;
  }
  winddir_avg2m = sum / WIND_DIR_AVG_SIZE;
  if(winddir_avg2m >= 360) winddir_avg2m -= 360;
  if(winddir_avg2m < 0) winddir_avg2m += 360;

  //Calc windgustmph_10m
```

```
  //Calc windgustdir_10m
  //Find the largest windgust in the last 10 minutes
  windgustmph_10m = 0;
  windgustdir_10m = 0;
  //Step through the 10 minutes
  for(int i = 0; i < 10 ; i++)
  {
    if(windgust_10m[i] > windgustmph_10m)
    {
      windgustmph_10m = windgust_10m[i];
      windgustdir_10m = windgustdirection_10m[i];
    }
  }

  //Calc humidity
  humidity = myHumidity.readHumidity();
  //float temp_h = myHumidity.readTemperature();
  //Serial.print(" TempH:");
  //Serial.print(temp_h, 2);

  //Calc tempf from pressure sensor
  tempf = myPressure.readTempF();
  //Serial.print(" TempP:");
  //Serial.print(tempf, 2);

  //Total rainfall for the day is calculated within the interrupt
  //Calculate amount of rainfall for the last 60 minutes
  rainin = 0;
  for(int i = 0 ; i < 60 ; i++)
    rainin += rainHour[i];

  //Calc pressure
  pressure = myPressure.readPressure();

  //Calc dewptf

  //Calc light level
  light_lvl = get_light_level();

  //Calc battery level
  batt_lvl = get_battery_level();
}

//Returns the voltage of the light sensor based on the 3.3V rail
//This allows us to ignore what VCC might be (an Arduino plugged into USB has VCC of 4.5 to 5.2V)
float get_light_level()
{
  float operatingVoltage = analogRead(REFERENCE_3V3);

  float lightSensor = analogRead(LIGHT);

  operatingVoltage = 3.3 / operatingVoltage; //The reference voltage is 3.3V

  lightSensor = operatingVoltage * lightSensor;

  return(lightSensor);
}

//Returns the voltage of the raw pin based on the 3.3V rail
```

```
//This allows us to ignore what VCC might be (an Arduino plugged into USB has VCC of 4.5 to 5.2V)
//Battery level is connected to the RAW pin on Arduino and is fed through two 5% resistors:
//3.9K on the high side (R1), and 1K on the low side (R2)
float get_battery_level()
{
  float operatingVoltage = analogRead(REFERENCE_3V3);

  float rawVoltage = analogRead(BATT);

  operatingVoltage = 3.30 / operatingVoltage; //The reference voltage is 3.3V

  rawVoltage = operatingVoltage * rawVoltage; //Convert the 0 to 1023 int to actual voltage on BATT
pin

  rawVoltage *= 4.90; //(3.9k+1k)/1k - multiple BATT voltage by the voltage divider to get actual system
voltage

  return(rawVoltage);
}

//Returns the instataneous wind speed
float get_wind_speed()
{
  float deltaTime = millis() - lastWindCheck; //750ms

  deltaTime /= 1000.0; //Covert to seconds

  float windSpeed = (float)windClicks / deltaTime; //3 / 0.750s = 4

  windClicks = 0; //Reset and start watching for new wind
  lastWindCheck = millis();

  windSpeed *= 1.492; //4 * 1.492 = 5.968MPH

  /* Serial.println();
   Serial.print("Windspeed:");
   Serial.println(windSpeed);*/

  return(windSpeed);
}

//Read the wind direction sensor, return heading in degrees
int get_wind_direction()
{
  unsigned int adc;

  adc = analogRead(WDIR); // get the current reading from the sensor

  // The following table is ADC readings for the wind direction sensor output, sorted from low to high.
  // Each threshold is the midpoint between adjacent headings. The output is degrees for that ADC
reading.
  // Note that these are not in compass degree order! See Weather Meters datasheet for more
information.

  if (adc < 380) return (113);
  if (adc < 393) return (68);
  if (adc < 414) return (90);
  if (adc < 456) return (158);
  if (adc < 508) return (135);
```

```
  if (adc < 551) return (203);
  if (adc < 615) return (180);
  if (adc < 680) return (23);
  if (adc < 746) return (45);
  if (adc < 801) return (248);
  if (adc < 833) return (225);
  if (adc < 878) return (338);
  if (adc < 913) return (0);
  if (adc < 940) return (293);
  if (adc < 967) return (315);
  if (adc < 990) return (270);
  return (-1); // error, disconnected?
}


//Prints the various variables directly to the port
//I don't like the way this function is written but Arduino doesn't support floats under sprintf
void printWeather()
{
  calcWeather(); //Go calc all the various sensors

  Serial.println();
  Serial.print("$,winddir=");
  Serial.print(winddir);
  Serial.print(",windspeedmph=");
  Serial.print(windspeedmph, 1);
  Serial.print(",windgustmph=");
  Serial.print(windgustmph, 1);
  Serial.print(",windgustdir=");
  Serial.print(windgustdir);
  Serial.print(",windspdmph_avg2m=");
  Serial.print(windspdmph_avg2m, 1);
  Serial.print(",winddir_avg2m=");
  Serial.print(winddir_avg2m);
  Serial.print(",windgustmph_10m=");
  Serial.print(windgustmph_10m, 1);
  Serial.print(",windgustdir_10m=");
  Serial.print(windgustdir_10m);
  Serial.print(",humidity=");
  Serial.print(humidity, 1);
  Serial.print(",tempf=");
  Serial.print(tempf, 1);
  Serial.print(",rainin=");
  Serial.print(rainin, 2);
  Serial.print(",dailyrainin=");
  Serial.print(dailyrainin, 2);
  Serial.print(",pressure=");
  Serial.print(pressure, 2);
  Serial.print(",batt_lvl=");
  Serial.print(batt_lvl, 2);
  Serial.print(",light_lvl=");
  Serial.print(light_lvl, 2);

  Serial.print(",lat=");
  Serial.print(gps.location.lat(), 6);
  Serial.print(",lat=");
  Serial.print(gps.location.lng(), 6);
  Serial.print(",altitude=");
  Serial.print(gps.altitude.meters());
```

```
  Serial.print(",sats=");
  Serial.print(gps.satellites.value());

   char sz[32];
  Serial.print(",date=");
  sprintf(sz, "%02d/%02d/%02d", gps.date.month(), gps.date.day(), gps.date.year());
  Serial.print(sz);

  Serial.print(",time=");
  sprintf(sz, "%02d:%02d:%02d", gps.time.hour(), gps.time.minute(), gps.time.second());
  Serial.print(sz);

  Serial.print(",");
  Serial.println("#");

}
```

APPENDIX Q.

PYTHOND CODE USED FOR STORING ARDUINO SERIAL MONITOR INFORMATION. MODIFIED FROM https://stackoverflow.com/questions/20892133/storing-string-from-arduino-to-text-file-using-python.

```
## import the serial library
import serial

## Boolean variable that will represent
## whether or not the arduino is connected
connected = False

## establish connection to the serial port that your arduino
## is connected to.

locations=['COM1','COM2','COM3','COM4','COM5','COM6','COM7','/dev/ttyUSB7']

for device in locations:
    try:
        print "Trying...",device
        ser = serial.Serial(device, 9600)
        break
    except:
        print "Failed to connect on",device

## loop until the arduino tells us it is ready
while not connected:
    serin = ser.readline()
    connected = True

## open text file to store the current
##gps co-ordinates received from the rover
text_file = open("position4.txt", 'w')
## read serial data from arduino and
## write it to the text file 'position.txt'
while 1:
    if ser.inWaiting():
        x=ser.readline()
        print(x)
        text_file.write(x)
        if x=="\n":
            text_file.seek(0)
```

```
            text_file.truncate()
        text_file.flush()

## close the serial connection and text file
text_file.close()
ser.close()
```

VITA

Matthew Benjamin Rogers

Candidate for the Degree of

Master of Science

Thesis: EVALUATION OF VARIOUS OPERATING PARAMETERS ON AGRICULTURAL BOOMLESS NOZZLE SPRAY PATTERNS

Major Field: Biosystems Engineering

Biographical:

Education:

Completed the requirements for the Master of Science in Biosystems Engineering at Oklahoma State University, Stillwater, Oklahoma in July, 2017.

Completed the requirements for the Bachelor of Science in Biosystems Engineering at Oklahoma State University, Stillwater, Oklahoma in 2015.

Experience:

Graduate Research Assistant, Oklahoma State University, 2015-2017

Professional Memberships:

American Society of Agricultural and Biological Engineers, 2012-2017